

Practical Circuitry for Measurement and Control Problems

Circuits Designed for a Cruel and Unyielding World

Jim Williams

INTRODUCTION

This collection of circuits was worked out between June 1991 and July of 1994. Most were designed at customer request or are derivatives of such efforts. All represent substantial effort and, as such, are disseminated here for wider study and (hopefully) use.¹ The examples are roughly arranged in categories including power conversion, transducer signal conditioning, amplifiers and signal generators. As always, reader comment and questions concerning variants of the circuits shown may be addressed directly to the author.

Clock Synchronized Switching Regulator

Gated oscillator type switching regulators permit high efficiency over extended ranges of output current. These regulators achieve this desirable characteristic by using a gated oscillator architecture instead of a clocked pulse width modulator. This eliminates the “housekeeping” cur-

rents associated with the continuous operation of fixed frequency designs. Gated oscillator regulators simply self-clock at whatever frequency is required to maintain the output voltage. Typically, loop oscillation frequency ranges from a few hertz into the kilohertz region, depending upon the load.

In most cases this asynchronous, variable frequency operation does not create problems. Some systems, however, are sensitive to this characteristic. Figure 1 slightly modifies a gated oscillator type switching regulator by synchronizing its loop oscillation frequency to the systems clock. In this fashion the oscillation frequency and its attendant switching noise, albeit variable, become coherent with system operation.

Note 1: “Study” is certainly a noble pursuit but we never fail to emphasize use.

LT and LTC are registered trademarks and LT is a trademark of Linear Technology Corporation.

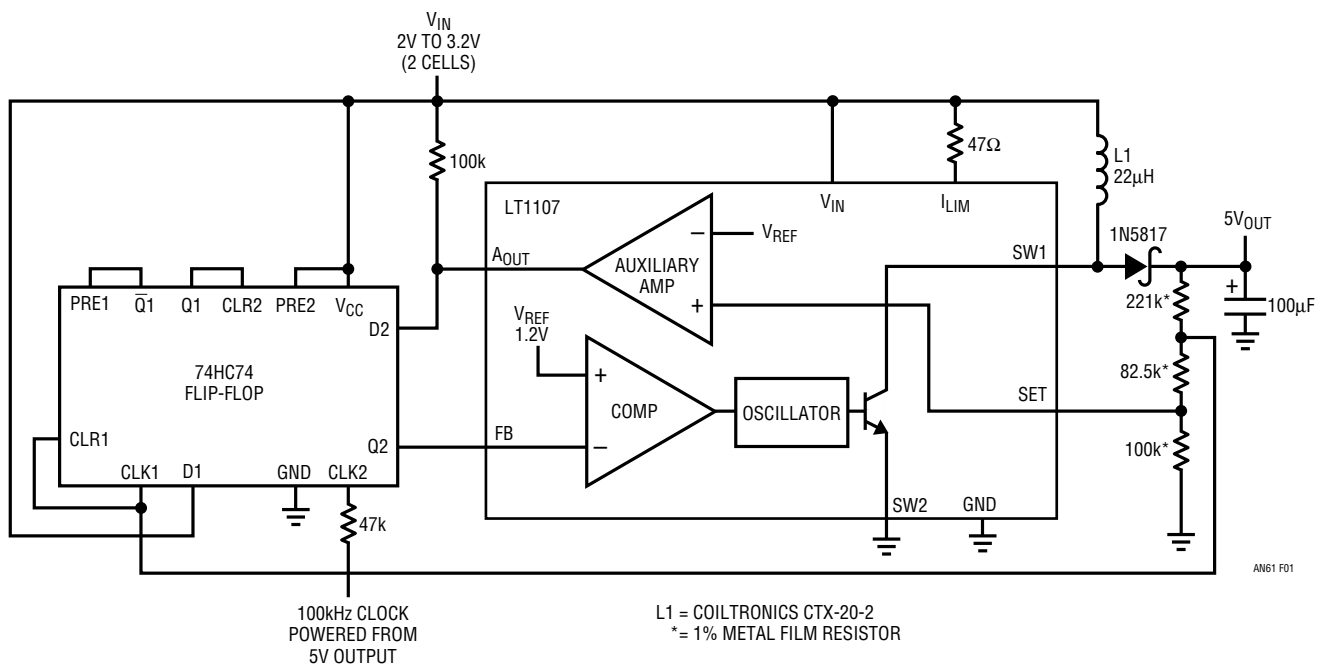


Figure 1. A Synchronizing Flip-Flop Forces Switching Regulator Noise to Be Coherent with the Clock

mechanism. The 1.5V powered LT1073 switching regulator forms a start-up loop. When power is applied the LT1073 runs, causing its V_{SW} pin to periodically pull current through L1. L1 responds with high voltage flyback events. These events are rectified and stored in the 470 μ F capacitor, producing the circuit's DC output. The output divider string is set up so the LT1073 turns off when circuit output crosses about 4.5V. Under these conditions the LT1073 obviously can no longer drive L1, but the LT1170 can. When the start-up circuit goes off, the LT1170 V_{IN} pin has adequate supply voltage and can operate. There is some overlap between start-up loop turn-off and LT1170 turn-on, but it has no detrimental effect.

The start-up loop must function over a wide range of loads and battery voltages. Start-up currents approach 1A, necessitating attention to the LT1073's saturation and drive characteristics. The worst case is a nearly depleted battery and heavy output loading.

Figure 4 plots input-output characteristics for the circuit. Note that the circuit will start into all loads with $V_{BAT} = 1.2V$. Start-up is possible down to 1.0V at reduced loads. Once the circuit has started, the plot shows it will drive full 200mA loads down to $V_{BAT} = 1.0V$. Reduced drive is possible down to $V_{BAT} = 0.6V$ (a very dead battery)! Figure 5 graphs efficiency at two supply voltages over a range of output currents. Performance is attractive, although at lower currents circuit quiescent power degrades efficiency. Fixed junction saturation losses are responsible for lower overall efficiency at the lower supply voltage.

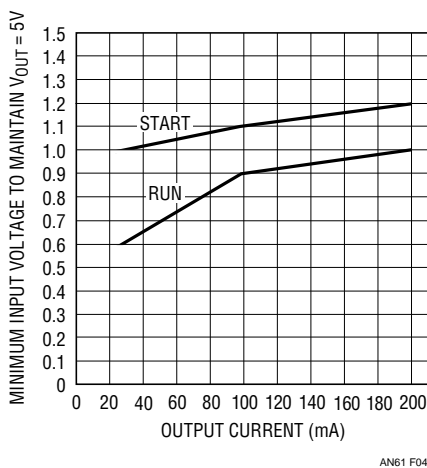


Figure 4. Input-Output Data for the 1.5V to 5V Converter Shows Extremely Wide Start-Up and Running Range into Full Load

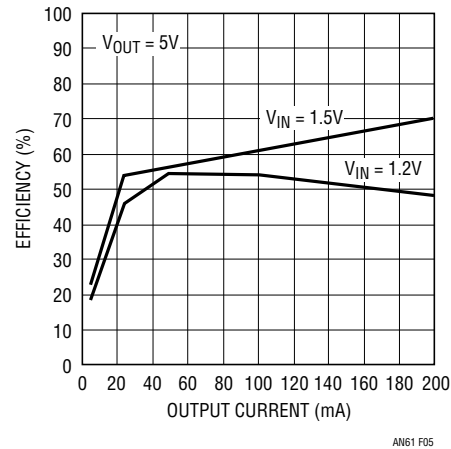


Figure 5. Efficiency vs Operating Point for the 1.5V to 5V Converter. Efficiency Suffers at Low Power Because of Relatively High Quiescent Currents

Low Power 1.5V to 5V Converter

Figure 6, essentially the same approach as the preceding circuit, was developed by Steve Pietkiewicz of LTC. It is limited to about 150mA output with commensurate restrictions on start-up current. Its advantage, good efficiency at relatively low output currents, derives from its low quiescent power consumption.

The LT1073 provides circuit start-up. When output voltage, sensed by the LT1073's "set" input via the resistor divider, rises high enough Q1 turns on, enabling the LT1302. This device sees adequate operating voltage and responds by driving the output to 5V, satisfying its feedback node. The 5V output also causes enough overdrive at the LT1073 feedback pin to shut the device down.

Figure 7 shows maximum permissible load currents for start-up and running conditions. Performance is quite good, although the circuit clearly cannot compete with the previous design. The fundamental difference between the two circuits is the LT1170's (Figure 3) much larger power switch, which is responsible for the higher available power. Figure 8, however, reveals another difference. The curves show that Figure 6 is significantly more efficient than the LT1170 based approach at output currents below 100mA. This highly desirable characteristic is due to the LT1302's much lower quiescent operating currents.

Application Note 61

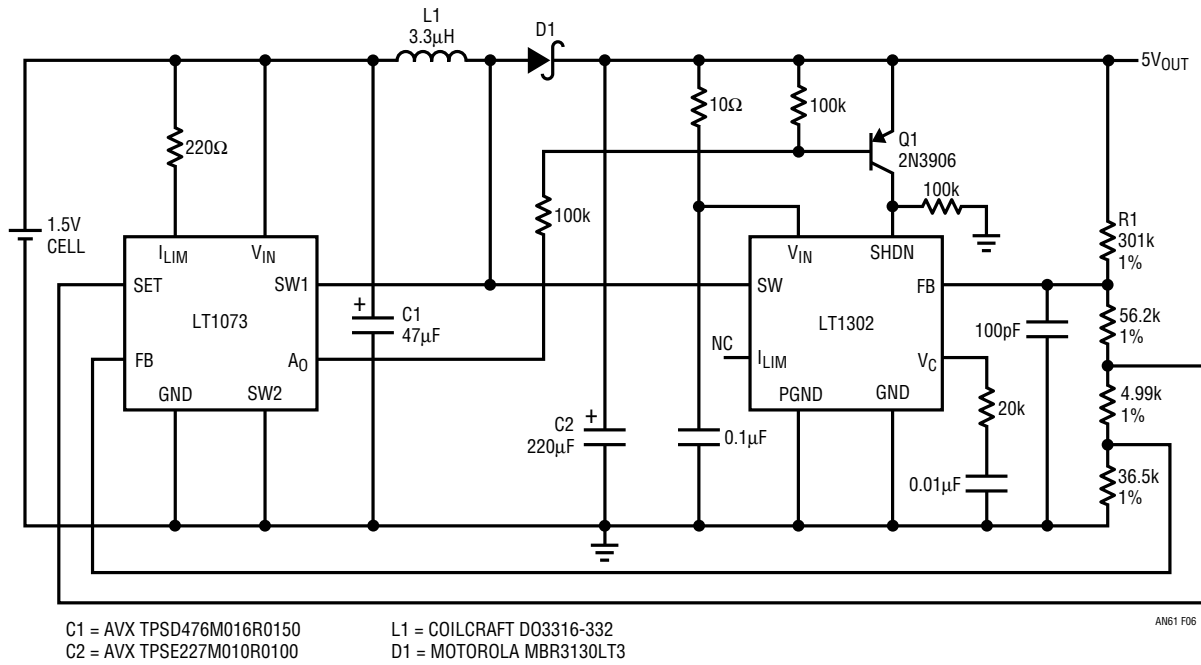


Figure 6. Single-Cell to 5V Converter Delivers 150mA with Good Efficiency at Lower Currents

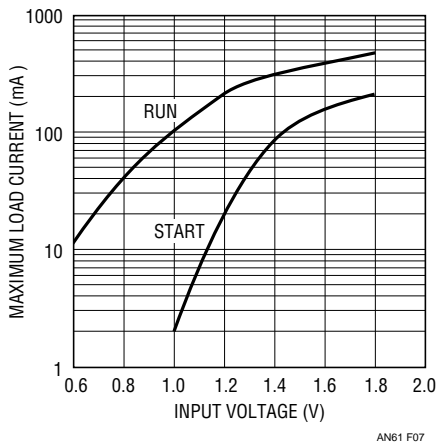


Figure 7. Maximum Permissible Loads for Start-Up and Running Conditions. Allowable Load Current During Start-Up Is Substantially Less Than Maximum Running Current.

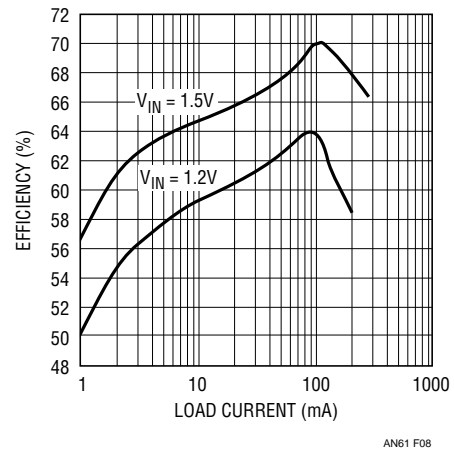


Figure 8. Efficiency Plot for Figure 6. Performance Is Better Than the Previous Circuit at Lower Currents, Although Poorer at High Power

Application Note 61

Circuit efficiency ranges from 80% to 88% at full load, depending on line voltage. Current mode operation combined with the Royer's consistent waveshape vs input results in excellent line rejection. The circuit has none of the line rejection problems attributable to the hysteretic voltage control loops typically found in low voltage micropower DC/DC converters. This is an especially desirable characteristic for CCFL control, where lamp intensity must remain constant with shifts in line voltage. Interaction between the Royer converter, the lamp and the regulation loop is far more complex than might be supposed, and subject to a variety of considerations. For detailed discussion see Reference 3.

Low Voltage Powered LCD Contrast Supply

Figure 10, a companion to the CCFL power supply previously described, is a contrast supply for LCD panels. It was designed by Steve Pietkiewicz of LTC. The circuit is noteworthy because it operates from a 1.8V to 6V input, significantly lower than most designs. In operation the LT1300/LT1301 switching regulator drives T1 in flyback

fashion, causing negative biased step-up at T1's secondary. D1 provides rectification, and C1 smooths the output to DC. The resistively divided output is compared to a command input, which may be DC or PWM, by the IC's "I_{LIM}" pin. The IC, forcing the loop to maintain 0V at the I_{LIM} pin, regulates circuit output in proportion to the command input.

Efficiency ranges from 77% to 83% as supply voltage varies from 1.8V to 3V. At the same supply limits, available output current increases from 12mA to 25mA.

HeNe Laser Power Supply

Helium-Neon lasers, used for a variety of tasks, are difficult loads for a power supply. They typically need almost 10kV to start conduction, although they require only about 1500V to maintain conduction at their specified operating currents. Powering a laser usually involves some form of start-up circuitry to generate the initial breakdown voltage and a separate supply for sustaining conduction. Figure 11's circuit considerably simplifies driving the laser. The

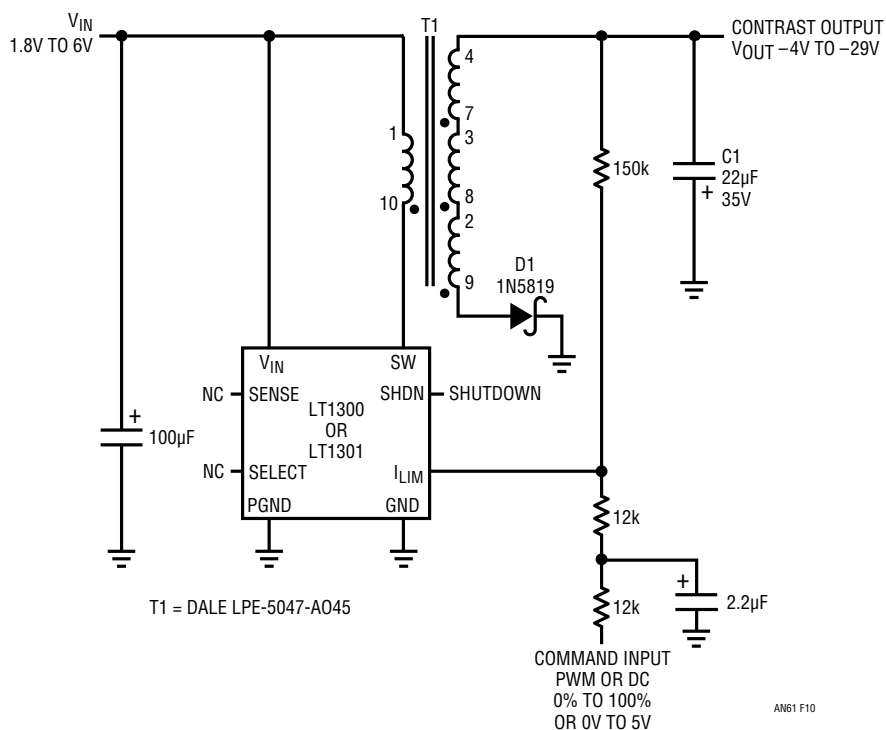


Figure 10. Liquid Crystal Display Contrast Supply Operates from 1.8V to 6V with -4V to -29V Output Range

start-up and sustaining functions have been combined into a single, closed-loop current source with over 10kV of compliance. The circuit is recognizable as a reworked CCFL power supply with a voltage tripled DC output.²

When power is applied, the laser does not conduct and the voltage across the 190Ω resistor is zero. The LT1170 switching regulator FB pin sees no feedback voltage, and its switch pin (V_{SW}) provides full duty cycle pulse width modulation to L2. Current flows from L1's center tap through Q1 and Q2 into L2 and the LT1170. This current flow causes Q1 and Q2 to switch, alternately driving L1. The 0.47μF capacitor resonates with L1, providing boosted sine wave drive. L1 provides substantial step-up, causing

about 3500V to appear at its secondary. The capacitors and diodes associated with L1's secondary form a voltage tripler, producing over 10kV across the laser. The laser breaks down and current begins to flow through it. The 47k resistor limits current and isolates the laser's load characteristic. The current flow causes a voltage to appear across the 190Ω resistor. A filtered version of this voltage appears at the LT1170 FB pin, closing a control loop. The LT1170 adjusts pulse width drive to L2 to maintain the FB pin at 1.23V, regardless of changes in operating conditions. In this fashion, the laser sees constant current drive,

Note 2: See References 2 and 3 and this text's Figure 9.

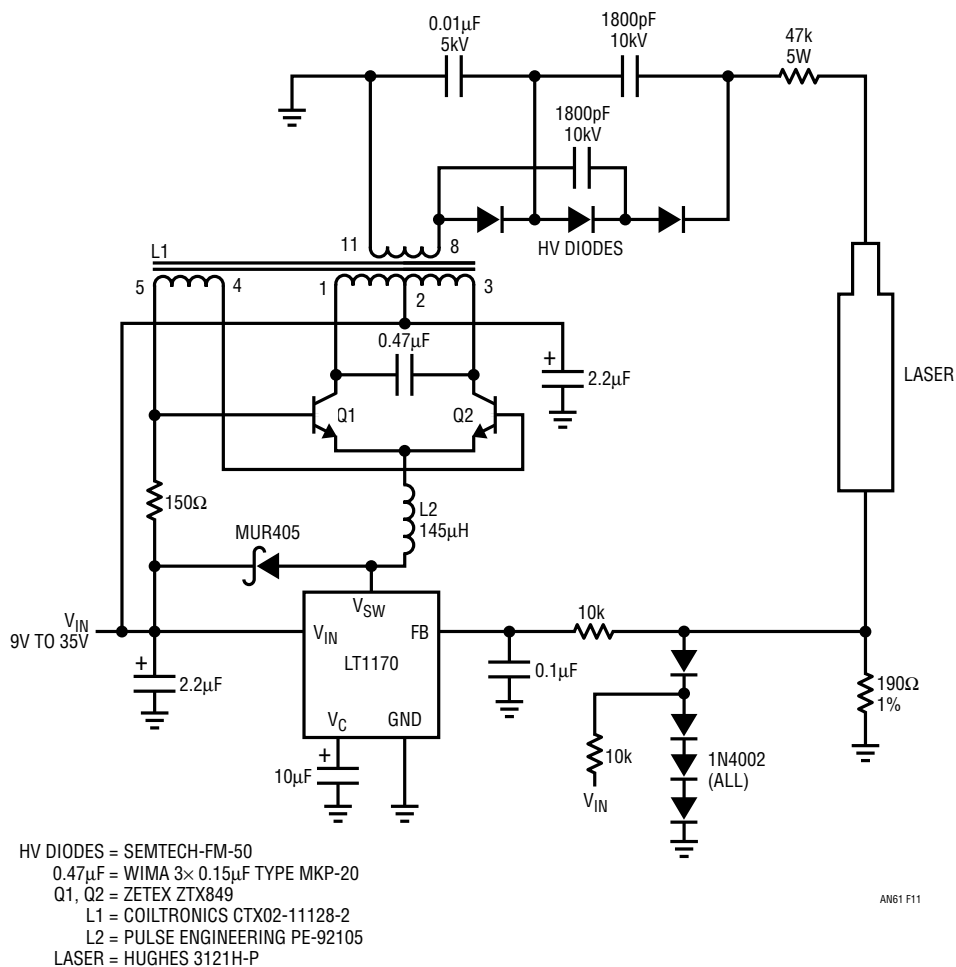


Figure 11. LASER Power Supply Is Essentially A 10,000V Compliance Current Source

Application Note 61

in this case 6.5mA. Other currents are obtainable by varying the 190Ω value. The 1N4002 diode string clamps excessive voltages when laser conduction first begins, protecting the LT1170. The 10μF capacitor at the V_C pin frequency compensates the loop and the MUR405 maintains L1's current flow when the LT1170 V_{SW} pin is not conducting. The circuit will start and run the laser over a 9V to 35V input range with an electrical efficiency of about 80%.

Compact Electroluminescent Panel Power Supply

Electroluminescent (EL) panel LCD backlighting presents an attractive alternative to fluorescent tube (CCFL) backlighting in some portable systems. EL panels are thin, lightweight, lower power, require no diffuser and work at lower voltage than CCFLs. Unfortunately, most EL DC/AC

inverters use a large transformer to generate the 400Hz 95V square wave required to drive the panel. Figure 12's circuit, developed by Steve Pietkiewicz of LTC, eliminates the transformer by employing an LT1108 micropower DC/DC converter IC. The device generates a 95VDC potential via L1 and the diode-capacitor doubler network. The transistors switch the EL panel between 95V and ground. C1 blocks DC and R1 allows intensity adjustment. The 400Hz square wave drive signal can be supplied by the microprocessor or a simple multivibrator. When compared to conventional EL panel supplies, this circuit is noteworthy because it can be built in a square inch with a 0.5 inch height restriction. Additionally, all components are surface mount types, and the usual large and heavy 400Hz transformer is eliminated.

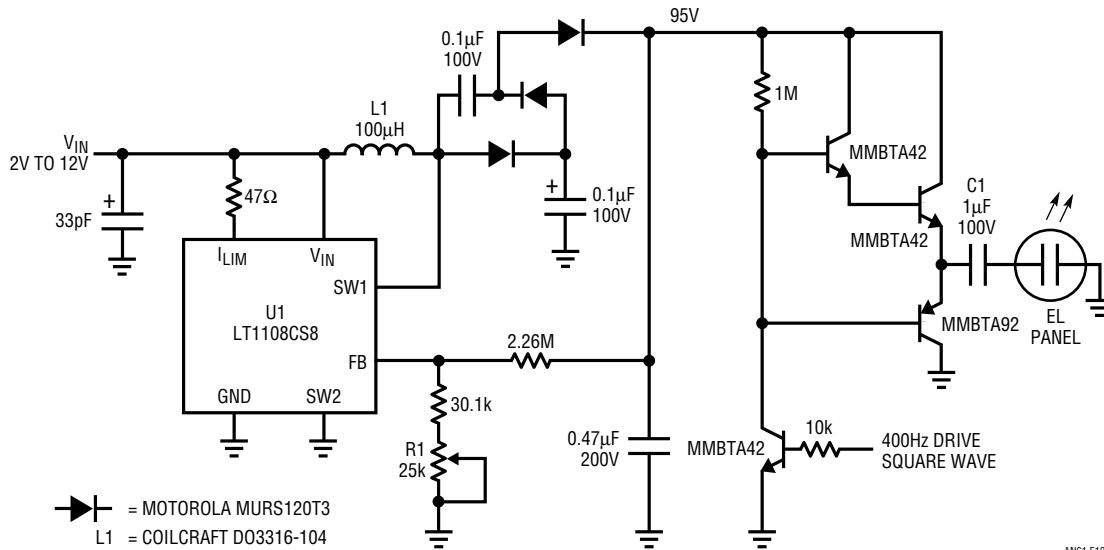


Figure 12. Switch Mode EL Panel Driver Eliminates Large 400Hz Transformer

3.3V Powered Barometric Pressure Signal Conditioner

The move to 3.3V digital supply voltage creates problems for analog signal conditioning. In particular, transducer based circuits often require higher voltage for proper transducer excitation. DC/DC converters in standard configurations can address this issue but increase power consumption. Figure 13's circuit shows a way to provide proper transducer excitation for a barometric pressure sensor while minimizing power requirements.

The 6kΩ transducer T1 requires precisely 1.5mA of excitation, necessitating a relatively high voltage drive. A1 senses T1's current by monitoring the voltage drop across the resistor string in T1's return path.

A1's output biases the LT1172 switching regulator's operating point, producing a stepped up DC voltage which appears as T1's drive and A2's supply voltage. T1's return current out of pin 6 closes a loop back at A1 which is slaved to the 1.2V reference. This arrangement provides the required high voltage drive ($\approx 10V$) while minimizing power consumption. This is so because the switching regulator produces only enough voltage to satisfy T1's current requirements. Instrumentation amplifier A2 and A3 provide gain and LTC1287 A/D converter gives a 12-bit digital output. A2 is bootstrapped off the transducer supply, enabling it to accept T1's common-mode voltage. Circuit current consumption is about 14mA. If the shutdown pin is driven high the switching regulator turns off, reducing

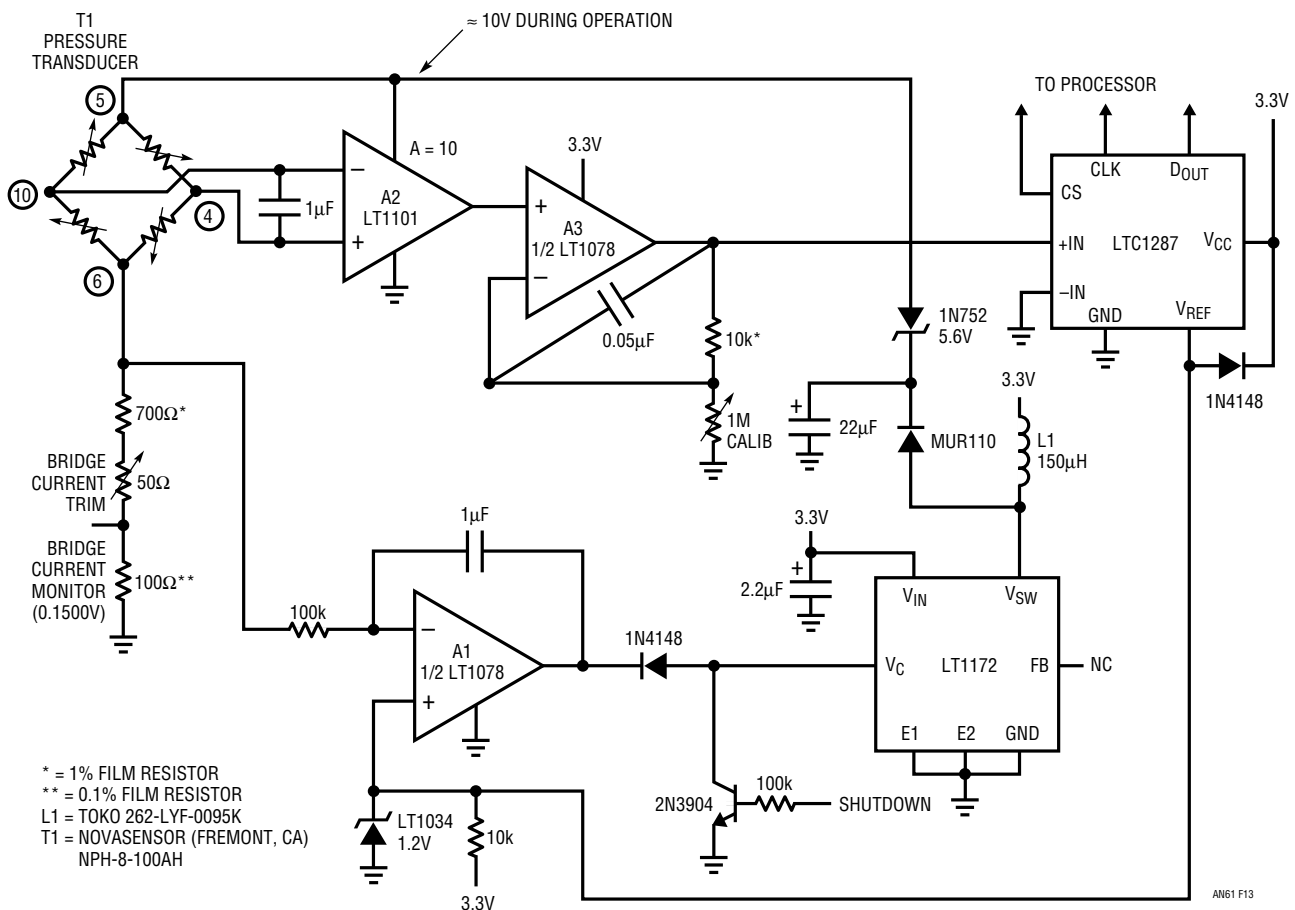


Figure 13. 3.3V Powered, Digital Output, Barometric Pressure Signal Conditioner

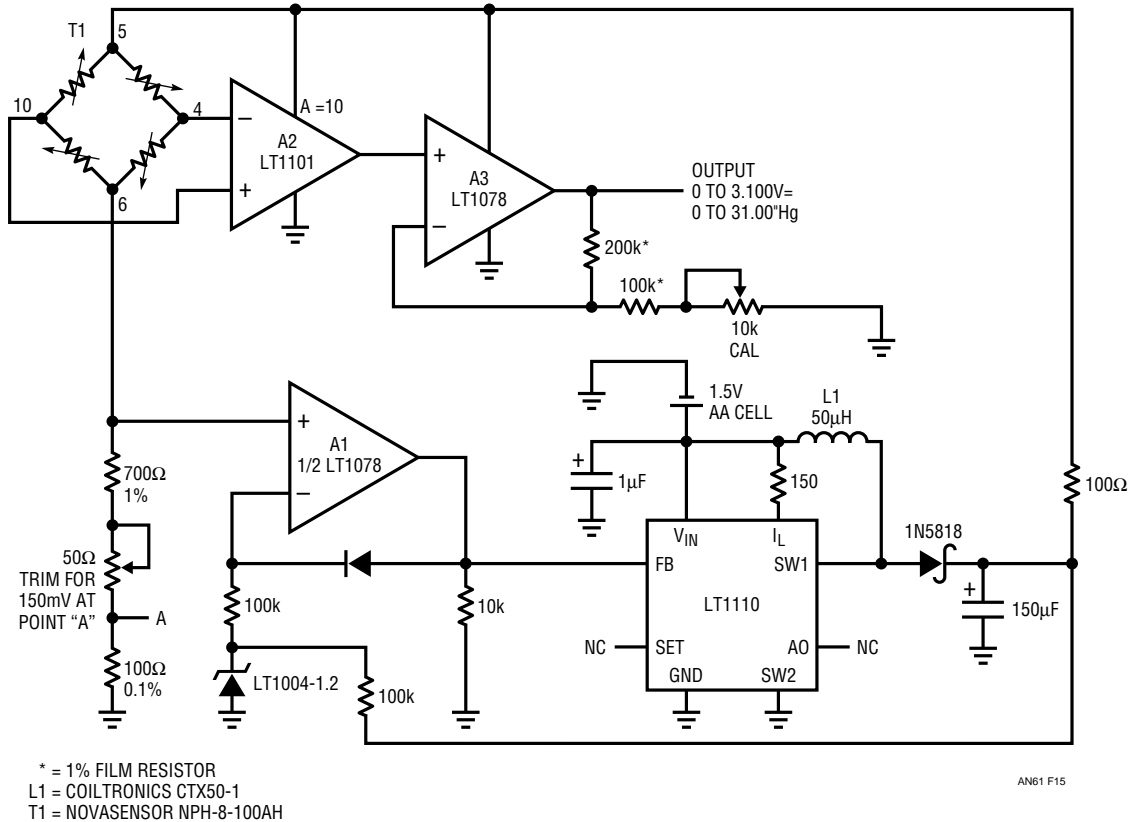


Figure 15. 1.5V Powered Barometric Pressure Signal Conditioner Uses Instrumentation Amplifier and Voltage Boosted Current Loop

output, in turn, closes a feedback loop at the regulator. This loop generates whatever voltage step-up is required to force precisely 1.5mA through T1. This arrangement provides the required high voltage drive while minimizing power consumption. This occurs because the switching regulator produces only enough voltage to satisfy T1's current requirements.

L1 pins 1 and 2 source a boosted, fully floating voltage, which is rectified and filtered. This potential powers A2. Because A2 floats with respect to T1, it can look differentially across T1's outputs, pins 10 and 4. In practice, pin 10 becomes "ground" and A2 measures pin 4's output with respect to this point. A2's gain-scaled output is the circuit's output, conveniently scaled at 3.000V = 30.00"Hg. A2's floating drive eliminates the requirement for an instrumentation amplifier, saving cost, power, space and error contribution.

To calibrate the circuit, adjust R1 for 150mV across the 100Ω resistor in T1's return path. This sets T1's current to the manufacturer's specified calibration point. Next, adjust R2 at a scale factor of 3.000V = 30.00"Hg. If R2 cannot capture the calibration, reselect the 200k resistor in series with it. If a pressure standard is not available, the transducer is supplied with individual calibration data, permitting circuit calibration.

This circuit, compared to a high-order pressure standard, maintained 0.01"Hg accuracy over months with widely varying ambient pressure shifts. Changes in pressure, particularly rapid ones, correlated quite nicely to changing weather conditions. Additionally, because 0.01"Hg corresponds to about 10 feet of altitude at sea level, driving over hills and freeway overpasses becomes quite interesting.

Until recently, this type of accuracy and stability has only been attainable with bonded strain gauge and capacitively-based transducers, which are quite expensive. As such, semiconductor pressure transducer manufacturers whose products perform at the levels reported are to be applauded. Although high quality semiconductor transducers are still not comparable to more mature technologies, their cost is low and they are vastly improved over earlier devices.

The circuit pulls 14mA from the battery, allowing about 250 hours operation from one D cell.

Quartz Crystal-Based Thermometer

Although quartz crystals have been utilized as temperature sensors (see Reference 5), there has been almost no widespread adaptation of this technology. This is primarily due to the lack of standard product quartz-based temperature sensors. The advantages of quartz-based sensors include simple signal conditioning, good stability and a direct, noise immune digital output almost ideally suited to remote sensing.

Figure 17 utilizes an economical, commercially available (see Reference 6) quartz-based temperature sensor in a thermometer scheme suited to remote data collection.

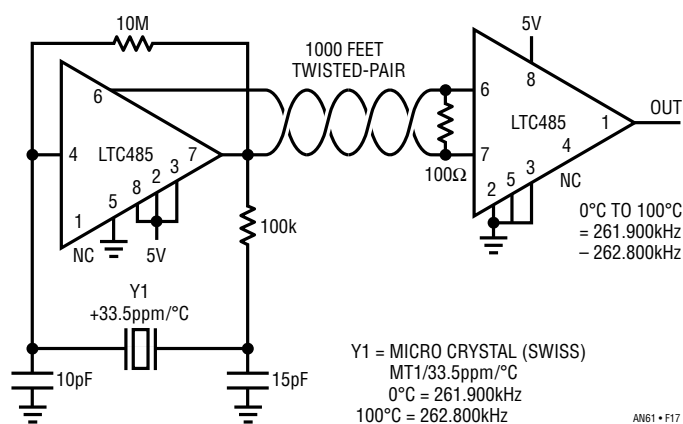


Figure 17. Quartz Crystal Based Circuit Provides Temperature-to-Frequency Conversion. RS485 Transceivers Allow Remote Sensing

The LTC485 RS485 transceiver is set up in the transmit mode. The crystal and discrete components combine with the IC's inverting gain to form a Pierce type oscillator. The LTC485's differential line driving outputs provide frequency coded temperature data to a 1000-foot cable run. A second RS485 transceiver differentially receives the data and presents a single-ended output. Accuracy depends on the grade of quartz sensor specified, with 1°C over 0°C to 100°C achievable.

Ultra-Low Noise and Low Drift Chopped-FET Amplifier

Figure 18's circuit combines the extremely low drift of a chopper-stabilized amplifier with a pair of low noise FETs. The result is an amplifier with 0.05 μ V/°C drift, offset within 5 μ V, 100pA bias current and 50nV noise in a 0.1Hz to 10Hz bandwidth. The noise performance is especially noteworthy; it is almost 35 times better than monolithic chopper-stabilized amplifiers and equals the best bipolar types.

FETs Q1 and Q2 differentially feed A2 to form a simple low noise op amp. Feedback, provided by R1 and R2, sets closed-loop gain (in this case 10,000) in the usual fashion. Although Q1 and Q2 have extraordinarily low noise characteristics, their offset and drift are uncontrolled. A1, a chopper-stabilized amplifier, corrects these deficiencies. It does this by measuring the difference between the amplifier's inputs and adjusting Q1's channel current via Q3 to minimize the difference. Q1's skewed drain values ensure that A1 will be able to capture the offset. A1 and Q3 supply whatever current is required into Q1's channel to force offset within 5 μ V. Additionally, A1's low bias current does not appreciably add to the overall 100pA amplifier bias current. As shown, the amplifier is set up for a noninverting gain of 10,000 although other gains and inverting operation are possible. Figure 19 is a plot of the measured noise performance.

The FETs' V_{GS} can vary over a 4:1 range. Because of this, they must be selected for 10% V_{GS} matching. This matching allows A1 to capture the offset without introducing any significant noise.

Application Note 61

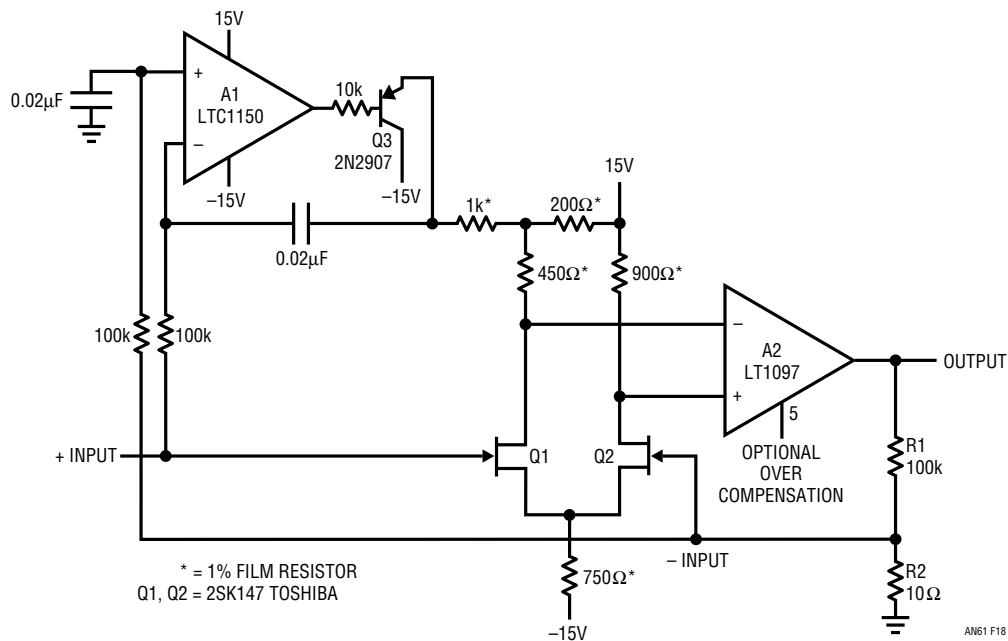


Figure 18. Chopper-Stabilized FET Pair Combines Low Bias, Offset and Drift with 45nV Noise

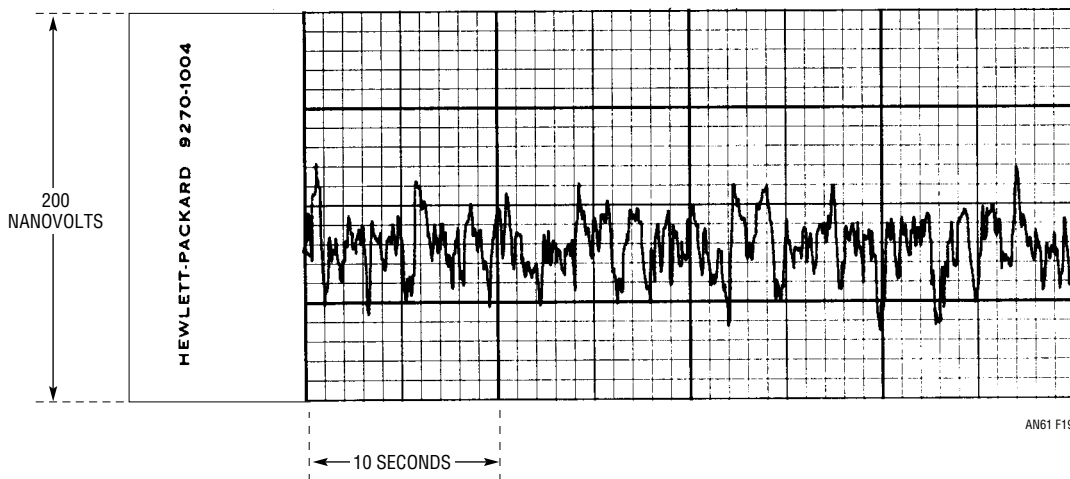


Figure 19. Figure 18's 45nV Noise Performance in a 0.1Hz to 10Hz Bandwidth. A1's Low Offset and Drift Are Retained, But Noise Is Almost 35 Times Better

Figure 20 shows the response (trace B) to a 1mV input step (trace A). The output is clean, with no overshoots or uncontrolled components. If A2 is replaced with a faster device (e.g., LT1055) speed increases by an order of magnitude with similar damping. A2's optional overcompensation can be used (capacitor to ground) to optimize response for low closed-loop gains.

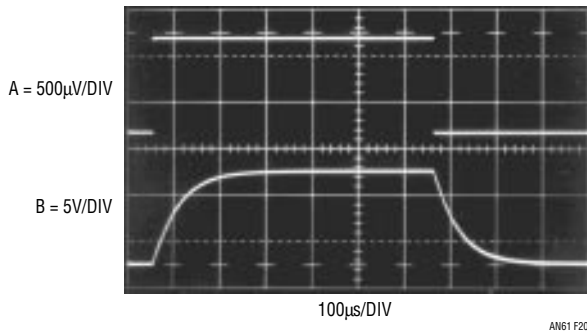


Figure 20. Step Response for the Low Noise $\times 10,000$ Amplifier. A $10\times$ Speed Increase Is Obtainable by Replacing A2 with a Faster Device

High Speed Adaptive Trigger Circuit

Line receivers often require an adaptive trigger to compensate for variations in signal amplitude and DC offsets. The circuit in Figure 21 triggers on 2mV to 100mV signals from 100Hz to 10MHz while operating from a single 5V rail. A1, operating at a gain of 20, provides wideband AC gain. The output of this stage biases a 2-way peak detector (Q1-Q4). The maximum peak is stored in Q2's emitter capacitor, while the minimum excursion is retained in Q4's emitter capacitor. The DC value of A1's output signal's midpoint appears at the junction of the 500pF capacitor and the 10M Ω units. This point always sits midway between the signal's excursions, regardless of absolute amplitude. This signal-adaptive voltage is buffered by A2 to set the trigger voltage at the LT1116's positive input. The LT1116's negative input is biased directly from A1's output. The LT1116's output, the circuit's output, is unaffected by 50:1 signal amplitude variations. Bandwidth limiting in A1 does not affect triggering because the adaptive trigger threshold varies ratiometrically to maintain circuit output.

Split supply versions of this circuit can achieve bandwidths to 50MHz with wider input operating range (See Reference 7).

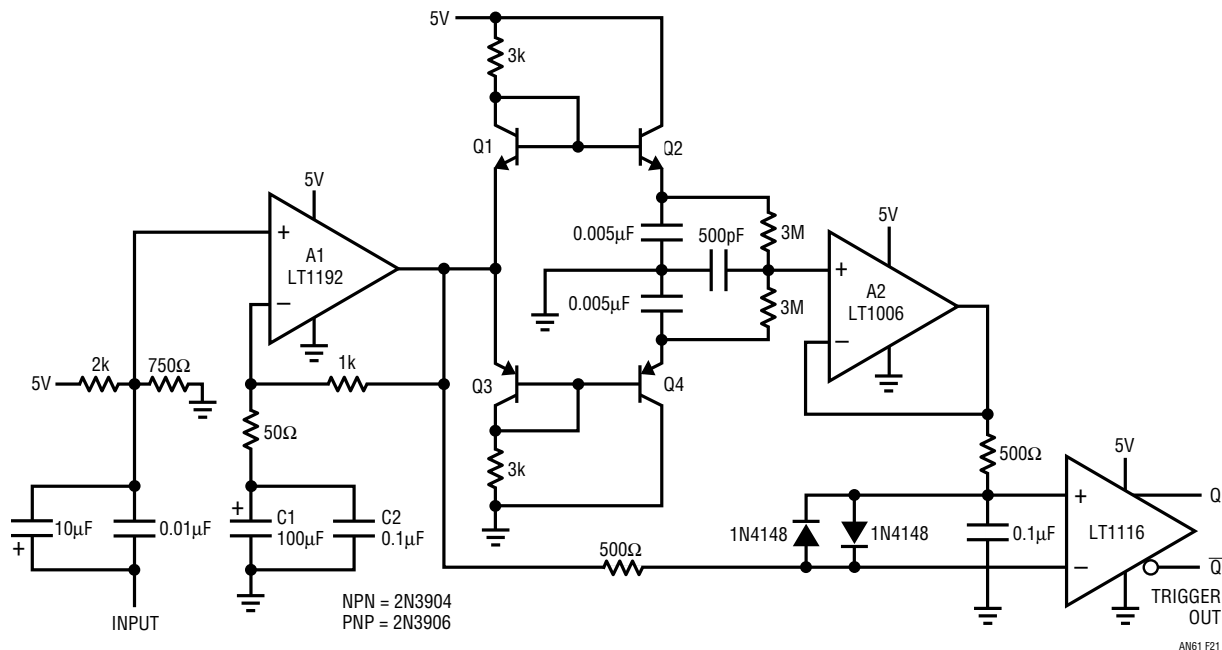


Figure 21. Fast Single Supply Adaptive Trigger. Output Comparator's Trip Level Varies Ratiometrically with Input Amplitude, Maintaining Data Integrity Over 50:1 Input Amplitude Range

Application Note 61

Wideband, Thermally-Based RMS/DC Converter

Applications such as wideband RMS voltmeters, RF leveling loops, wideband AGC, high crest factor measurements, SCR power monitoring and high frequency noise measurements require wideband, true RMS/DC conversion. The thermal conversion method achieves vastly higher bandwidth than any other approach. Thermal RMS/DC converters are direct acting, thermoelectronic analog computers. The thermal technique is explicit, relying on “first principles,” e.g., a waveforms RMS value is defined as its heating value in a load.

Figure 22 is a wideband, thermally-based RMS/DC converter.³ It provides a true RMS/DC conversion from DC to 10MHz with less than 1% error, regardless of input signal waveshape. It also features high input impedance and overload protection.

The circuit consists of three blocks; a wideband FET input amplifier, the RMS/DC converter and overload protection. The amplifier provides high input impedance, gain and drives the RMS/DC converters input heater. Input resistance is defined by the 1M resistor with input capacitance about 3pF. Q1 and Q2 constitute a simple, high speed FET input buffer. Q1 functions as a source follower, with the Q2 current source load setting the drain-source channel current. The LT1206 provides a flat 10MHz bandwidth gain of ten. Normally, this open-loop configuration would be quite drifts because there is no DC feedback. The LT1097 contributes this function to stabilize the circuit. It does this by comparing the filtered circuit output to a similarly filtered version of the input signal. The amplified difference between these signals is used to set Q2's bias, and hence Q1's channel current. This forces Q1's V_{GS} to whatever voltage is required to match the circuit's input and output potentials. The capacitor at A1 provides stable

loop compensation. The RC network in A1's output prevents it from seeing high speed edges coupled through Q2's collector-base junction. Q4, Q5 and Q6 form a low leakage clamp which precludes A1 loop latch-up during start-up or overdrive conditions. This can occur if Q1 ever forward biases. The 5K-50pF network gives A2 a slight peaking characteristic at the highest frequencies, allowing 1% flatness to 10MHz. A2's output drives the RMS/DC converter.

The LT1088 based RMS/DC converter is made up of matched pairs of heaters and diodes and a control amplifier. The LT1206 drives R1, producing heat which lowers D1's voltage. Differentially connected A3 responds by driving R2, via Q3, to heat D2, closing a loop around the amplifier. Because the diodes and heater resistors are matched, A3's DC output is related to the RMS value of the input, regardless of input frequency or waveshape. In practice, residual LT1088 mismatches necessitate a gain trim, which is implemented at A4. A4's output is the circuit output. The LT1004 and associated components frequency compensate the loop and provide good settling time over wide ranges of operating conditions (see Footnote 3).

Start-up or input overdrive can cause A2 to deliver excessive current to the LT1088 with resultant damage. C1 and C2 prevent this. Overdrive forces D1's voltage to an abnormally low potential. C1 triggers low under these conditions, pulling C2's input low. This causes C2's output to go high, putting A2 into shutdown and terminating the overload. After a time determined by the RC at C2's input, A2 will be enabled. If the overload condition still exists the loop will almost immediately shut A2 down again. This oscillatory action will continue, protecting the LT1088 until the overload condition is removed.

Note 3: Thermally based RMS/DC conversion is detailed in Reference 9.

Application Note 61

Performance for the circuit is quite impressive. Figure 23 plots error from DC to 11MHz. The graph shows 1% error bandwidth of 11MHz. The slight peaking out to 5MHz is due to the gain boost network at A2's negative input. The peaking is minimal compared to the total error envelope, and a small price to pay to get the 1% accuracy to 10MHz.

To trim this circuit put the 5k Ω potentiometer at its maximum resistance position and apply a 100 mV, 5MHz signal. Trim the 500 Ω adjustment for exactly 1V_{OUT}. Next, apply a 5MHz 1V input and trim the 10k potentiometer for 10.00V_{OUT}. Finally, put in 1V at 10MHz and adjust the 5k Ω trimmer for 10.00V_{OUT}. Repeat this sequence until circuit output is within 1% accuracy for DC-10MHz inputs. Two passes should be sufficient.

It is worth considering that this circuit performs the same function as instruments costing thousands of dollars.⁴

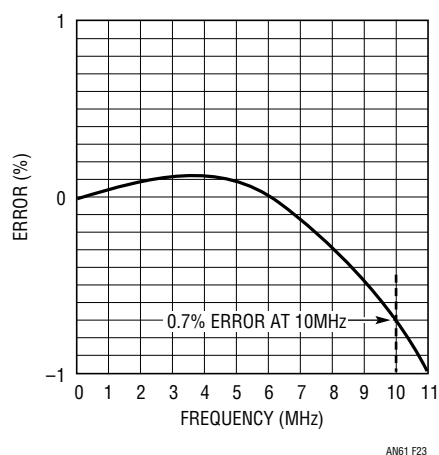


Figure 23. Error Plot for the RMS/DC Converter. Frequency Dependent Gain Boost at A2 Preserves 1% Accuracy, But Causes Slight Peaking Before Roll-Off

Hall Effect Stabilized Current Transformer

Current transformers are common and convenient. They permit wideband current measurement independent of common-mode voltage considerations. The most conve-

Note 4: Viewed from a historical perspective it is remarkable that so much precision wideband performance is available from such a relatively simple configuration. For perspective, see Appendix A, "Precision Wideband Circuitry . . . Then and Now."

nient current transformers are the "clip-on" type, commercially sold as "current probes." A problem with all simple current transformers is that they cannot sense DC and low frequency information. This problem was addressed in the mid-1960's with the advent of the Hall effect stabilized current probe. This approach uses a Hall effect device within the transformer core to sense DC and low frequency signals. This information is combined with the current transformers output to form a composite DC-to-high frequency output. Careful roll-off and gain matching of the two channels preserves amplitude accuracy at all frequencies.⁵ Additionally, the low frequency channel is operated as a "force-balance," meaning that the low frequency amplifier's output is fed back to magnetically bias the transformer flux to zero. Thus, the Hall effect device does not have to respond linearly over wide ranges of current and the transformer core never sees DC bias, both advantageous conditions. The amount of DC and low frequency information is obtained at the amplifier's output, which corresponds to the bias needed to offset the measured current.

Figure 24 shows a practical circuit. The Hall effect transducer lies within the core of the clip-on current transformer specified. A very simplistic way to model the Hall generator is as a bridge, excited by the two 619 Ω resistors. The Hall generator's outputs (the midpoints of the "bridge") feed differential input transconductance amplifier A1, which takes gain, with roll-off set by the 50 Ω , 0.02 μ F RC at its output. Further gain is provided by A2, in the same package as A1. A current buffer provides power gain to drive the current transformers secondary. This connection closes a flux nulling loop in the transducer core. The offset adjustments should be set for 0V output with no current flowing in the clip-on transducer. Similarly, the loop gain and bandwidth trims should be set so that the composite output (the combined high and low frequency output across the grounded 50 Ω resistor) has clean step response and correct amplitude from DC to high frequency.

Note 5: Details of this scheme are nicely presented in Reference 15. Additional relevant commentary on parallel path schemes appears in Reference 7.

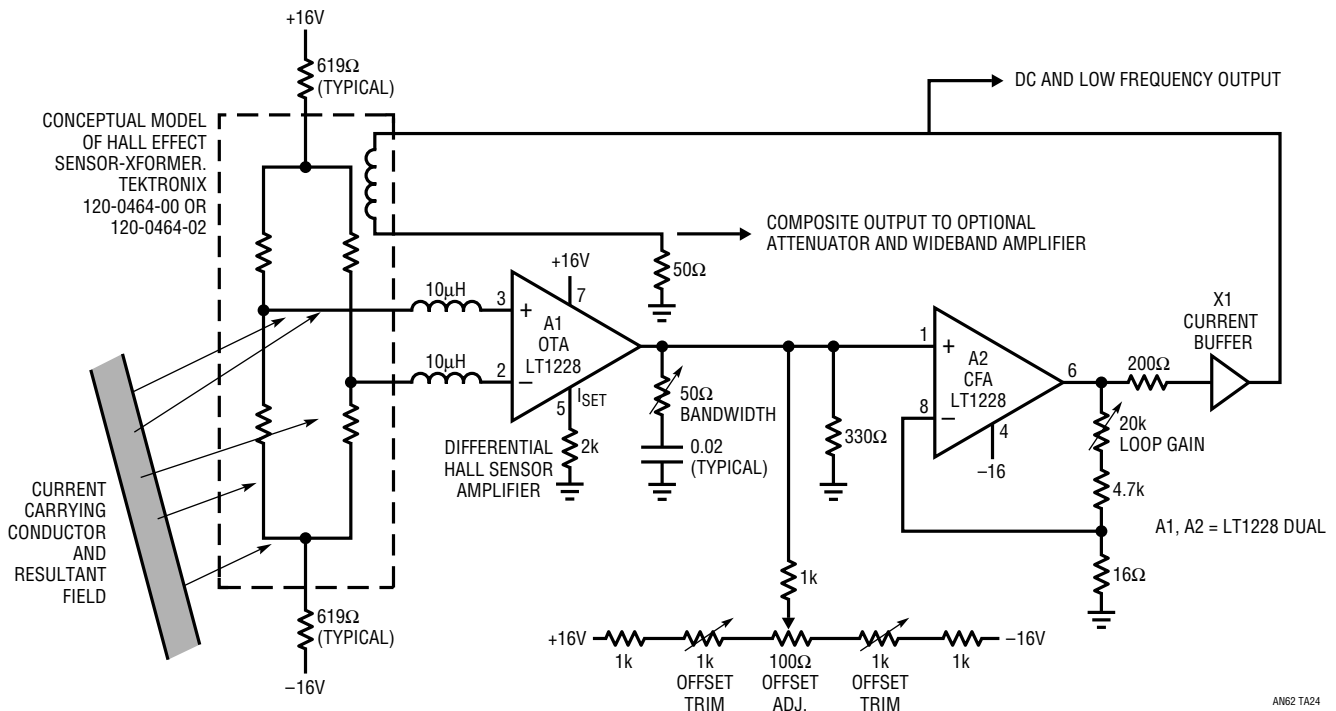


Figure 24. Hall Effect Stabilized Current Transformer (DC → High Frequency Current Probe)

Figure 25 shows a practical way to conveniently evaluate this circuit's performance. This partial schematic of the Tektronix P-6042 current probe shows a similar signal conditioning scheme for the transducer specified in Figure 24. In this case Q22, Q24 and Q29 combine with differential stage M-18 to form the Hall amplifier. To evaluate Figure 24's circuit remove M-18, Q22, Q24 and Q29. Next,

connect LT1228 pins 3 and 2 to the former M-18 pins 2 and 10 points, respectively. The $\pm 16V$ supplies are available from the P-6042's power bus. Also, connect the right end of Figure 24's 200Ω resistor to what was Q29's collector node. Finally, perform the offset, loop gain and bandwidth trims as previously described.

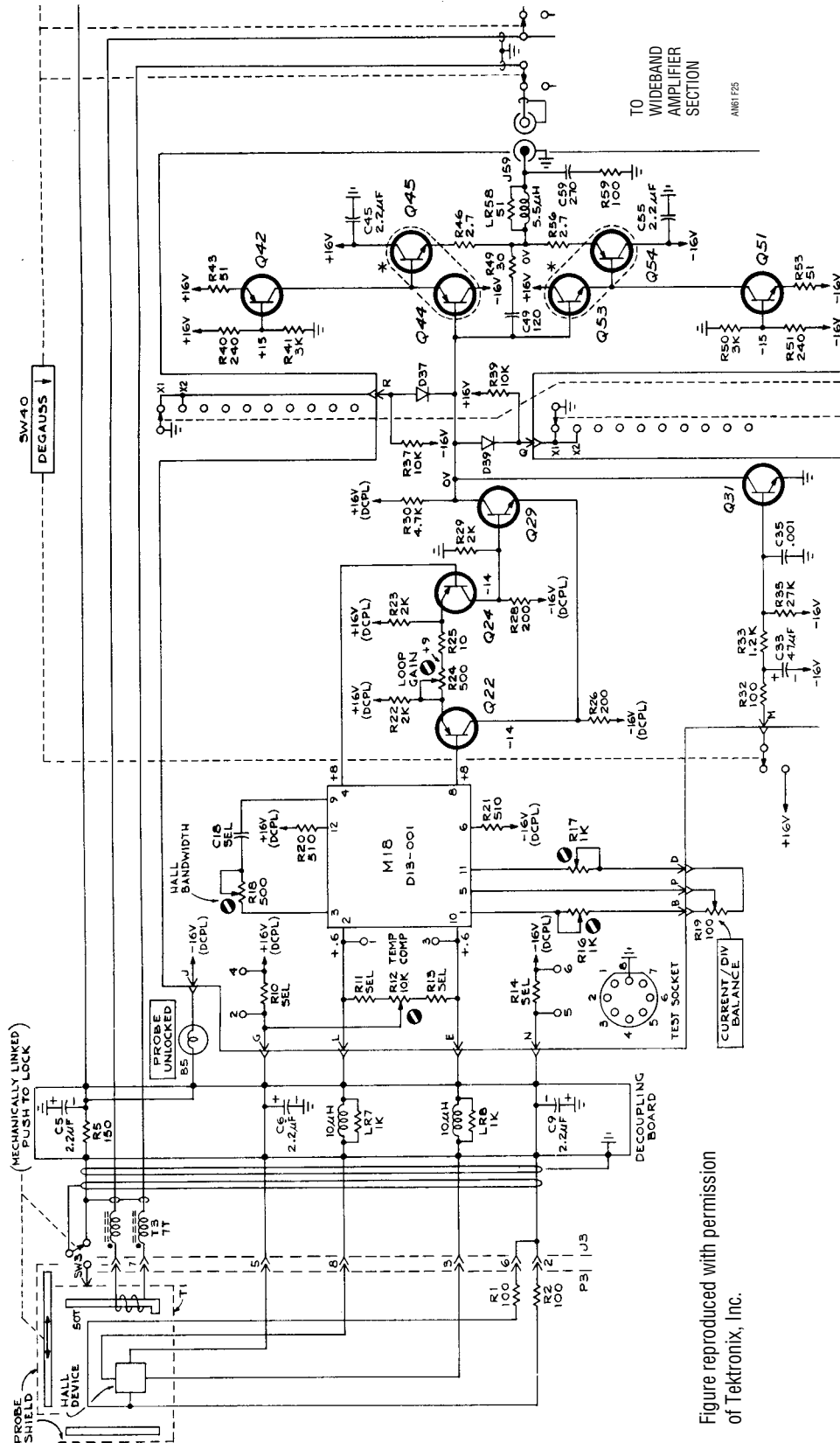


Figure reproduced with permission of Tektronix, Inc.

Figure 25. Tektronix P-6042 Hall Effect Based Current Probe Servo Loop.
Figure 24 Replaces M18 Amplifier and Q22, Q24 and Q29

Triggered 250 Picosecond Rise Time Pulse Generator

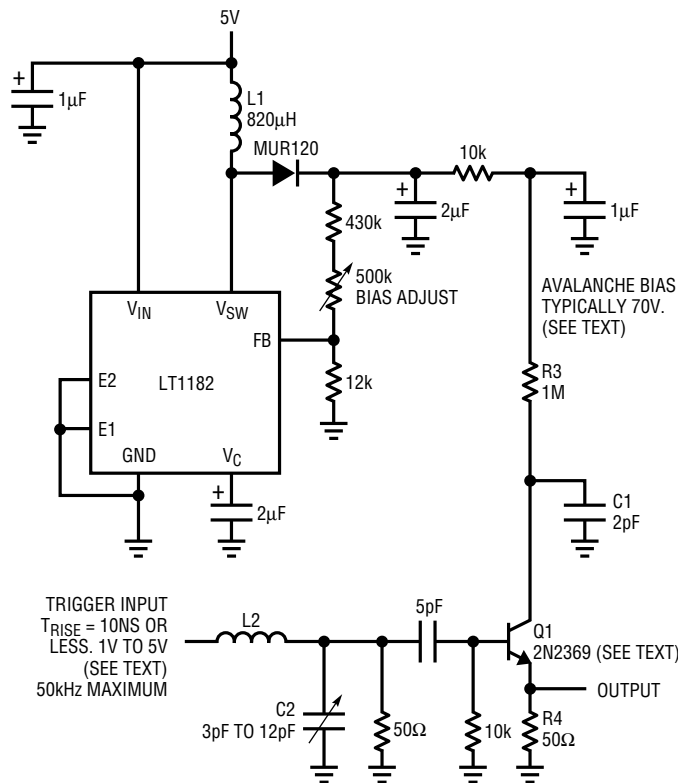
Verifying the rise time limit of wideband test equipment setups is a difficult task. In particular, the “end-to-end” rise time of oscilloscope-probe combinations is often required to assure measurement integrity. Conceptually, a pulse generator with rise times substantially faster than the oscilloscope-probe combination can provide this information. Figure 26’s circuit does this, providing an 800ps pulse with rise and fall times inside 250ps. Pulse amplitude is 10V with a 50Ω source impedance. This circuit has similarities to a previously published design (see Reference 7) except that it is triggered instead of free running. This feature permits synchronization to a clock or other event. The output phase with respect to the trigger is variable from 200ps to 5ns.

The pulse generator requires high voltage bias for operation. The LT1182 switching regulator forms a high voltage switched mode control loop. The LT1182 pulse

width modulates at its 100kHz clock rate. L1’s inductive events are rectified and stored in the 2μF output capacitor. The adjustable resistor divider provides feedback to the LT1182. The 10k-1μF RC provides noise filtering.

The high voltage is applied to Q1, a 40V breakdown device, via the R3-C1 combination. The high voltage “bias adjust” control should be set at the point where free running pulses across R4 *just* disappear. This puts Q1 slightly below its avalanche point. When an input trigger pulse is applied Q1 avalanches. The result is a quickly rising, very fast pulse across R4. C1 discharges, Q1’s collector voltage falls and breakdown ceases. C1 then recharges to just below the avalanche point. At the next trigger pulse this action repeats.⁶

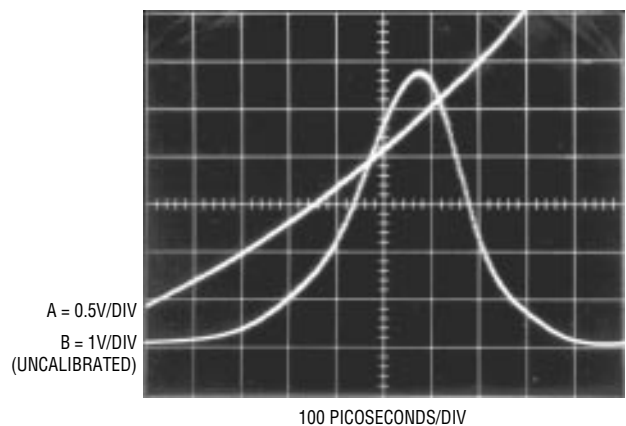
Figure 27 shows waveforms. A 3.9GHz sampling oscilloscope (Tektronix 661 with 4S2 sampling pug-in) measures the pulse (trace B) at 10V high with an 800ps base. Rise time is 250ps, with fall time indicating 200ps. The times are probably slightly faster, as the oscilloscope’s 90ps rise time influences the measurement.⁷ The input trigger pulse is trace A. Its amplitude provides a convenient way to vary the delay time between the trigger and output pulses. A 1V to 5V amplitude setting produces a continuous 5ns to 200ps delay range.



L1 = J.W. MILLER # 100267
L2 = 1 TURN # 28 WIRE, 1/4" TOTAL LENGTH

AN62 F26

Figure 26. Triggered 250ps Rise Time Pulse Generator. Trigger Pulse Amplitude Controls Output Phase



AN61 F27

Figure 27. Input Pulse Edge (Trace A) Triggers the Avalanche Pulse Output (Trace B). Display Granularity Is Characteristic of Sampling Oscilloscope Operation

Note 6: This circuit is based on the operation of the Tektronix Type 111 Pulse Generator. See Reference 16.

Note 7: I’m sorry, but 3.9GHz is the fastest ‘scope in my house (as of September, 1993).

Application Note 61

Some special considerations are required to optimize circuit performance. L2's very small inductance combines with C2 to slightly retard the trigger pulse's rise time. This prevents significant trigger pulse artifacts from appearing at the circuit's output. C2 should be adjusted for the best compromise between output pulse rise time and purity. Figure 28 shows partial pulse rise with C2 properly adjusted. There are no discernible discontinuities related to the trigger event.

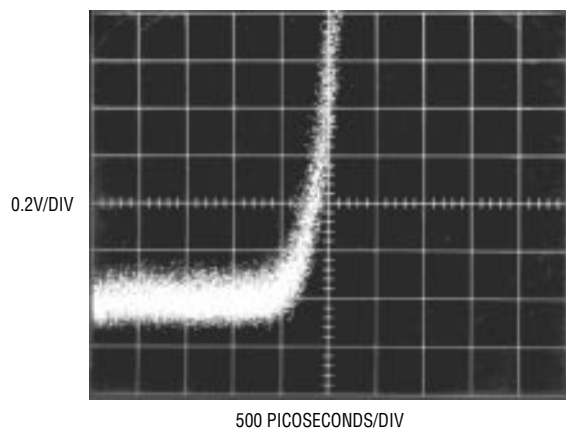


Figure 28. Expanded Scale View of Leading Edge Is Clean with No Trigger Pulse Artifacts. Display Granularity Derives from Sampling Oscilloscope Operation

Q1 may require selection to get avalanche behavior. Such behavior, while characteristic of the device specified, is not guaranteed by the manufacturer. A sample of 50 Motorola 2N2369s, spread over a 12 year date code span, yielded 82%. All "good" devices switched in less than 600ps. C1 is selected for a 10V amplitude output. Value spread is typically 2pF to 4pF. Ground plane type construction with high speed layout, connection and termination techniques are essential for a good results from this circuit.

Flash Memory Programmer

Although "Flash" type memory is increasingly popular, it does require some special programming features. The 5V powered memories need a carefully controlled 12V "VPP" programming pulse. The pulse's amplitude must be within 5% to assure proper operation. Additionally, the pulse must not overshoot, as memory destruction may occur for VPP outputs above 14V.⁸ These requirements usually

mandate a separate 12V supply and pulse forming circuitry. Figure 29's circuit provides the complete flash memory programming function with a single IC and some discrete components. All components are surface mount types, so little board space is required. The entire function runs off a single 5V supply.

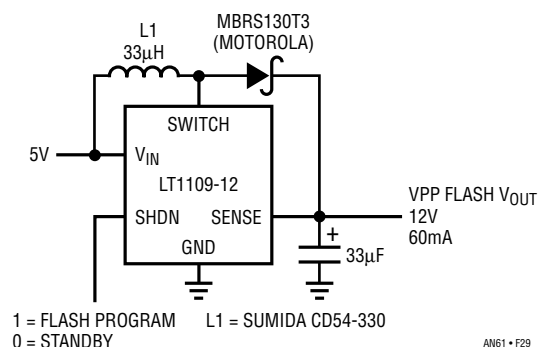


Figure 29. Switching Regulator Provides Complete Flash Memory Programmer

The LT1109-12 switching regulator functions by repetitively pulsing L1. L1 responds with high voltage flyback events, which are rectified by the diode and stored in the 10µF capacitor. The "sense" pin provides feedback, and the output voltage stabilizes at 12V within a few percent. The regulator's "shutdown" pin provides a way to control the VPP programming voltage output. With a logical zero applied to the pin the regulator shuts down, and no VPP programming voltage appears at the output. When the pin goes high (trace A, Figure 30) the regulator is activated, producing a cleanly rising, controlled pulse at the output (trace B). When the pin is returned to logical zero, the output smoothly decays off. The switched mode delivery of power combined with the output capacitor's filtering prevents overshoot while providing the required pulse amplitude accuracy. Trace C, a time and amplitude expanded version of trace B, shows this. The output steps up in amplitude each time L1 dumps energy into the output capacitor. When the regulation point is reached the amplitude cleanly flattens out, with only about 75mV of regulator ripple.

Note 8: See Reference 17 for detailed discussion.

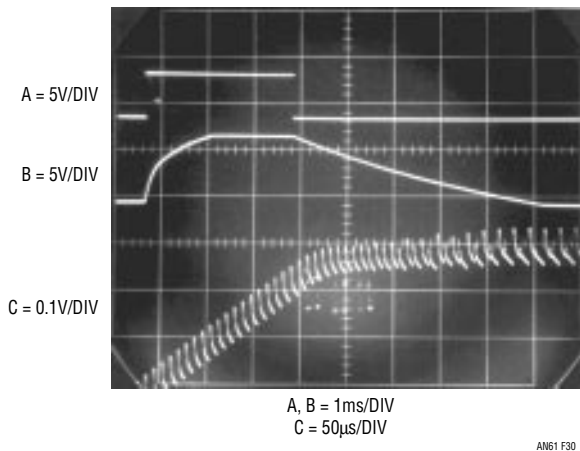


Figure 30. Flash Memory Programmer Waveforms Show Controlled Edges. Trace C Details Rise Time Settling

3.3V Powered V/F Converter

Figure 31 is a “charge pump” type V/F converter specifically designed to run from a 3.3V rail.⁹ A 0V to 2V input produces a corresponding 0kHz to 3kHz output with linearity inside 0.05%. To understand how the circuit works assume that A1’s negative input is just below 0V. The amplifier output is positive. Under these conditions, LTC1043’s pins 12 and 13 are shorted as are pins 11 and 7, allowing the 0.01 μ F capacitor (C1) to charge to the 1.2V LT1034 reference. When the input-voltage-derived current ramps A1’s summing point (negative input-trace A, Figure 32) positive, its output (trace B) goes low. This reverses the LTC1043’s switch states, connecting pins 12 and 14, and 11 and 8. This effectively connects C1’s positively charged end to ground on pin 8, forcing current to flow from A1’s summing junction into C1 via LTC1043 pin 14 (pin 14’s current is trace C). This action resets A1’s summing point to a small negative potential (again, trace A). The 120pF-50k-10k time constant at A1’s positive input ensures A1 remains low long enough for C1 to completely discharge (A1’s positive input is trace D). The Schottky diode prevents excessive negative excursions due to the 120pF capacitors differentiated response.

When the 120pF positive feedback path decays, A1’s output returns positive and the entire cycle repeats. The oscillation frequency of this action is directly related to the input voltage.

This is an AC coupled feedback loop. Because of this, start-up or overdrive conditions could force A1 to go low and

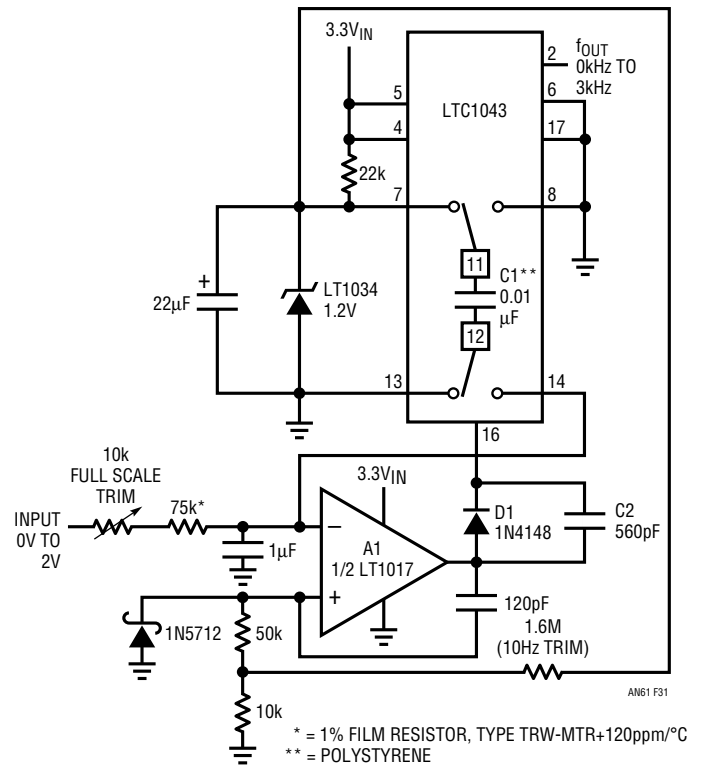


Figure 31. 3.3V Powered Voltage-to-Frequency Converter. Charge Pump Based Feedback Maintains High Linearity and Stability

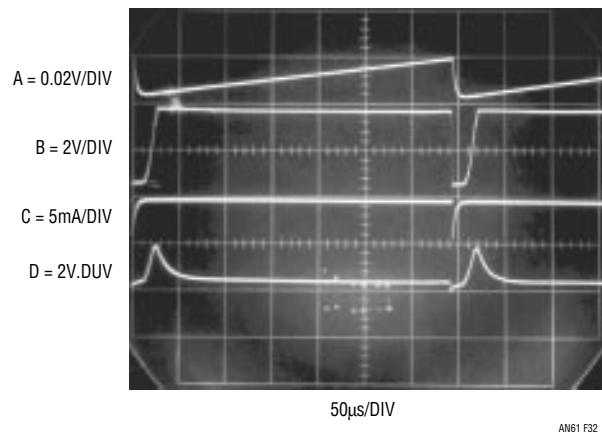


Figure 32. Waveform for the 3.3V Powered V/F. Charge Pump Action (Trace C) Maintains Summing Point (Trace A), Enforcing High Linearity and Accuracy

Note 9: See Reference 20 for a survey of V/F techniques.

ductance amplifier. A3's output feeds LT1228 A4, a current feedback amplifier. A4's output, also the circuit's output, is sampled by the A5-based gain control configuration. This closes a gain control loop to A3. A3's set current controls gain, allowing overall output level control.

Figure 34 shows noise at 1MHz bandpass, with Figure 35 showing RMS noise versus frequency in the same bandpass. Figure 36 plots similar information at full bandwidth (5MHz). RMS output is essentially flat to 1.5MHz with about ± 2 dB control to 5MHz before sagging badly.

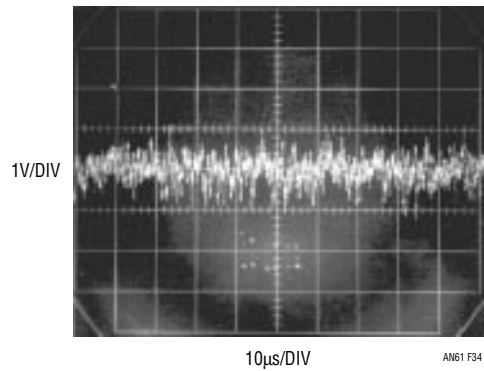


Figure 34. Figure 33's Output in the 1MHz Filter Position

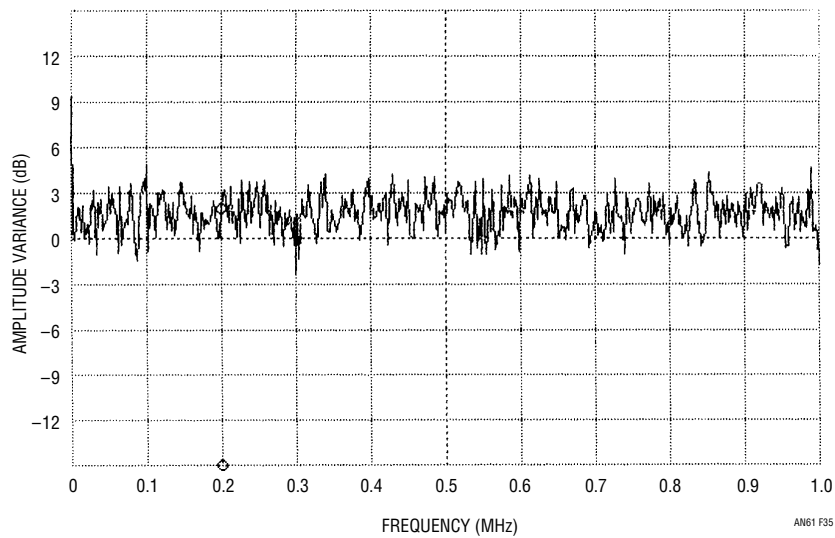


Figure 35. Amplitude vs Frequency for the Random Noise Generator Is Essentially Flat to 1MHz

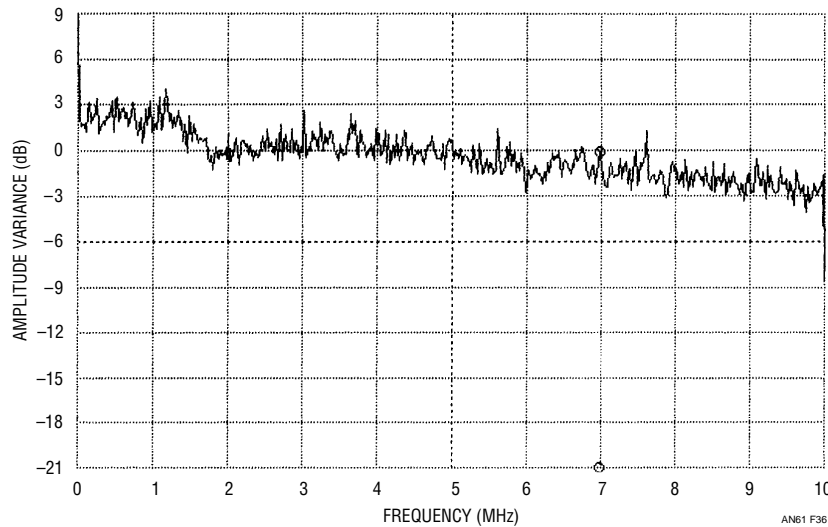


Figure 36. RMS Noise vs Frequency at 5MHz Bandpass Shows Slight Fall-Off Beyond 1MHz

Application Note 61

Figure 37's similar circuit substitutes a standard zener for the noise source but is more complex and requires a trim. A1, biased from the LT1004 reference, provides optimum drive for D1, the noise source. AC coupled A2 takes a broadband gain of 100. A2's output feeds a gain-control stage via a simple selectable lowpass filter. The filter's output is applied to LT1228 A3, an operational transconductance amplifier. A3's output feeds LT1228 A4, a current feedback amplifier. A4's output, the circuit's output,

is sampled by the A5-based gain control configuration. This closes a gain control loop back at A3. A3's set input current controls its gain, allowing overall output level control.

To adjust this circuit, place the filter in the 1kHz position and trim the 5k potentiometer for maximum negative bias at A3, pin 5.

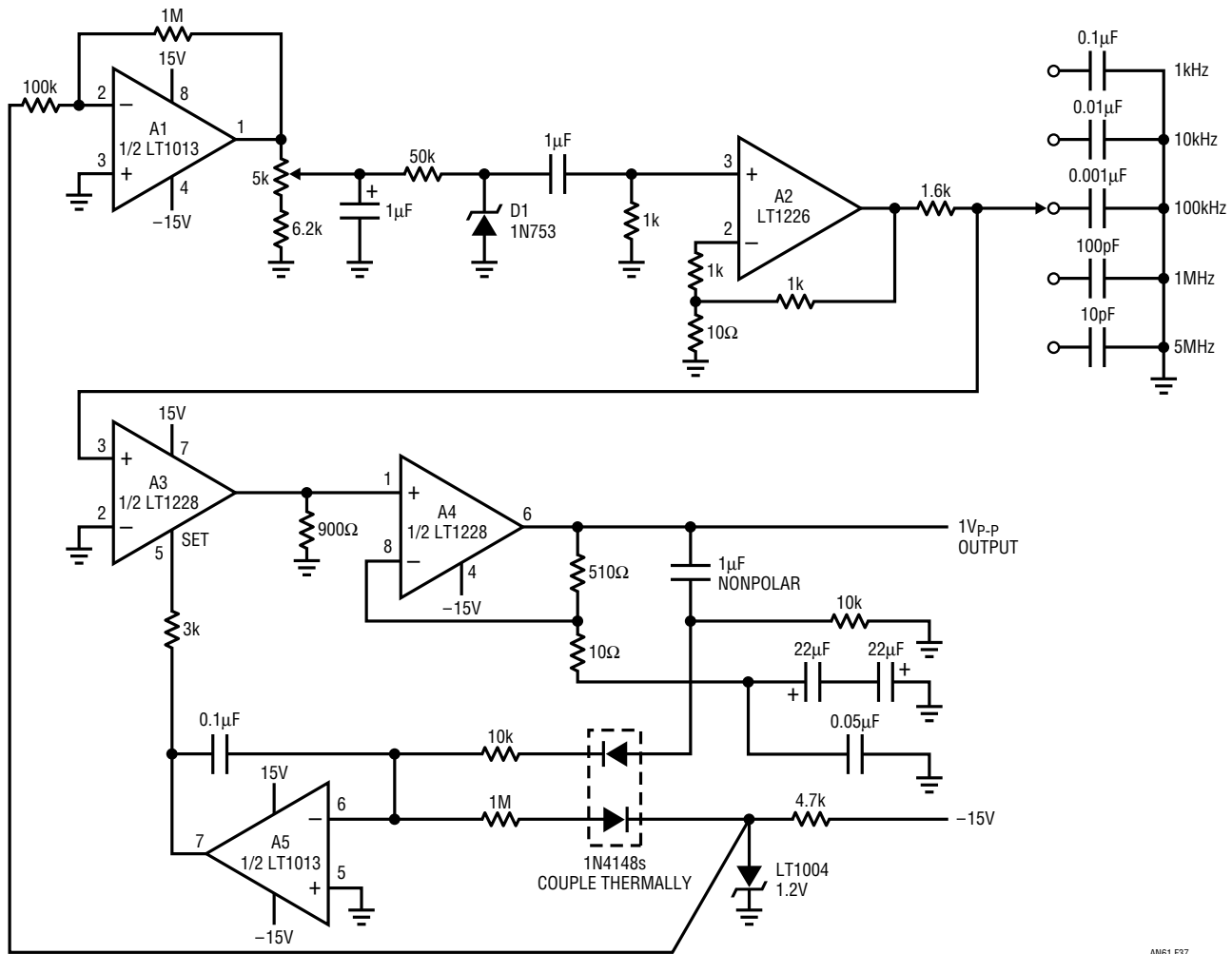


Figure 37. A Similar Circuit Uses a Standard Zener Diode, But Is More Complex and Requires Trimming

Switchable Output Crystal Oscillator

Figure 38's simple crystal oscillator circuit permits crystals to be electronically switched by logic commands. The circuit is best understood by initially ignoring all crystals. Further, assume all diodes are shorts and their associated 1k resistors open. The resistors at the LT1116's positive input set a DC bias point. The 2k-25pF path sets up phase shifted feedback and the circuit looks like a wideband unity gain follower at DC. When "Xtal A" is inserted (remember, D1 is temporarily shorted) positive feedback occurs and

oscillation commences at the crystals resonant frequency. If D1 and its associated 1k value are realized, oscillation can only continue if logic input A is biased high. Similarly, additional crystal-diode-1k branches permit logic selection of crystal frequency.

For AT cut crystals about a millisecond is required for the circuit output to stabilize due to the high Q factors involved. Crystal frequencies can be as high as 16MHz before comparator delays preclude reliable operation.

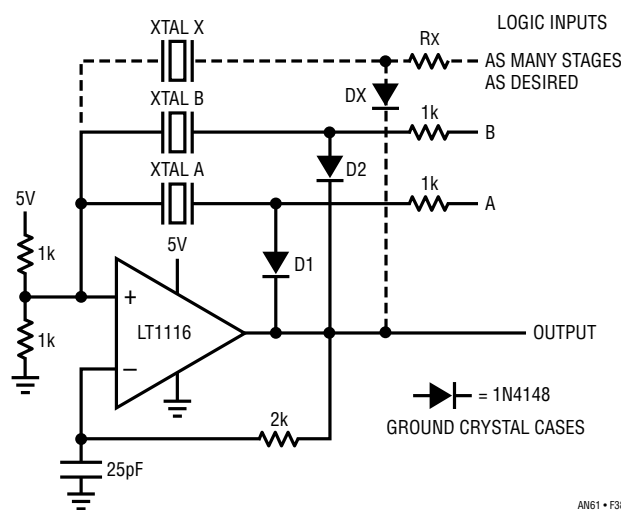


Figure 38. Switchable Output Crystal Oscillator. Biasing A or B High Places the Associated Crystal in the Feedback Path. Additional Crystal Branches Are Permissible

REFERENCES

- Williams, Jim and Huffman, Brian. "Some Thoughts on DC-DC Converters," pages 13-17, "1.5V to 5V Converters." Linear Technology Corporation, *Application Note 29*, October 1988.
- Williams, J., "Illumination Circuitry for Liquid Crystal Displays," Linear Technology Corporation, *Application Note 49*, August 1992.
- Williams, J., "Techniques for 92% Efficient LCD Illumination," Linear Technology Corporation, *Application Note 55*, August 1993.
- Williams, J., "Measurement and Control Circuit Collection," Linear Technology Corporation, *Application Note 45*, June 1991.
- Benjaminson, Albert, "The Linear Quartz Thermometer—a New Tool for Measuring Absolute and Difference Temperatures," *Hewlett-Packard Journal*, March 1965.
- Micro Crystal-ETA Fabriques d'Ebauches., "Miniature Quartz Resonators - MT Series" Data Sheet. 2540 Grenchen, Switzerland.

Application Note 61

7. Williams, J., "High Speed Amplifier Techniques," Linear Technology Corporation, *Application Note 47*, August 1991.
8. Williams, Jim, "High Speed Comparator Techniques," Linear Technology Corporation, *Application Note 13*, April 1985.
9. Williams, Jim, "A Monolithic IC for 100MHz RMS-DC Conversion," Linear Technology Corporation, *Application Note 22*, September 1987.
10. Ott, W.E., "A New Technique of Thermal RMS Measurement," *IEEE Journal of Solid State Circuits*, December 1974.
11. Williams, J.M. and Longman, T.L., "A 25MHz Thermally Based RMS-DC Converter," *1986 IEEE ISSCC Digest of Technical Papers*.
12. O'Neill, P.M., "A Monolithic Thermal Converter," *H.P. Journal*, May 1980.
13. C. Kitchen, L. Counts, "RMS-to-DC Conversion Guide," Analog Devices, Inc. 1986.
14. Tektronix, Inc. "P6042 Current Probe Operating and Service Manual," 1967.
15. Weber, Joe, "Oscilloscope Probe Circuits," Tektronix, Inc., Concept Series. 1969.
16. Tektronix, Inc., *Type 111 Pretrigger Pulse Generator Operating and Service Manual*, Tektronix, Inc. 1960.
17. Williams, J., "Linear Circuits for Digital Systems," Linear Technology Corporation, *Application Note 31*, February 1989.
18. Williams, J., "Applications for a Switched-Capacitor Instrumentation Building Block," Linear Technology Corporation, *Application Note 3*, July 1985.
19. Williams, J., "Circuit Techniques for Clock Sources," Linear Technology Corporation, *Application Note 12*, October 1985.
20. Williams, J. "Designs for High Performance Voltage-to-Frequency Converters," Linear Technology Corporation, *Application Note 14*, March 1986.

APPENDIX A

Precision Wideband Circuitry . . . Then and Now

Text Figure 22's relatively straightforward design provides a sensitive, thermally-based RMS/DC conversion to 10MHz with less than 1% error. Viewed from a historical perspective it is remarkable that so much precision wideband performance is so easily achieved.

Thirty years ago these specifications presented an extremely difficult engineering challenge, requiring deep-seated knowledge of fundamentals, extraordinary levels of finesse and an interdisciplinary outlook to achieve success.

The Hewlett-Packard model HP3400A (1965 price \$525 . . . about 1/3 the yearly tuition at M.I.T.) thermally-based RMS voltmeter included all of Figure 22's elements, but considerably more effort was required in its execution.¹ Our comparative study begins by considering H-P's version of Figure 22's FET buffer and precision wideband amplifier. The text is taken directly from the *HP3400A Operating and Service Manual*.²

Note 1: We are all constantly harangued about the advances made in computers since the days of the IBM360. This section gives analog aficionados a stage for their own bragging rights. Of course, an HP3400A was much more interesting than an IBM360 in 1965. Similarly, Figure 22's

capabilities are more impressive than any contemporary computer I'm aware of.

Note 2: All Hewlett-Packard text and figures used here are copyright 1965 Hewlett-Packard Company. Reproduced with permission.,

4-15. IMPEDANCE CONVERTER ASSEMBLY A2.

4-17. The ac signal input to the impedance converter is RC coupled to the grid of cathode follower V201³ through C201 and R203. The output signal is developed by Q201 which acts as a variable resistance in the cathode circuit of V201. The bootstrap feedback from the cathode of V201 to R203 increases the effective resistance of R203 to the input signal. This prevents R203 from loading the input signal and preserves the high input impedance of the Model 3400A. The gain compensating feedback from the plate of V201 to the base of Q201 compensates for any varying gain in V201 due to age or replacement.

4-18. Breakdown diode CR201 controls the grid bias voltage on V201 thereby establishing the operating point of this stage. CR202 and R211 across the base-emitter junction of Q201 protects Q201 in the event of a failure in the +75 volt power supply. Regulated dc is supplied to V201 filaments to avoid inducing ac hum in the signal path. This also prevents the gain of V201 changing with line voltage variations.

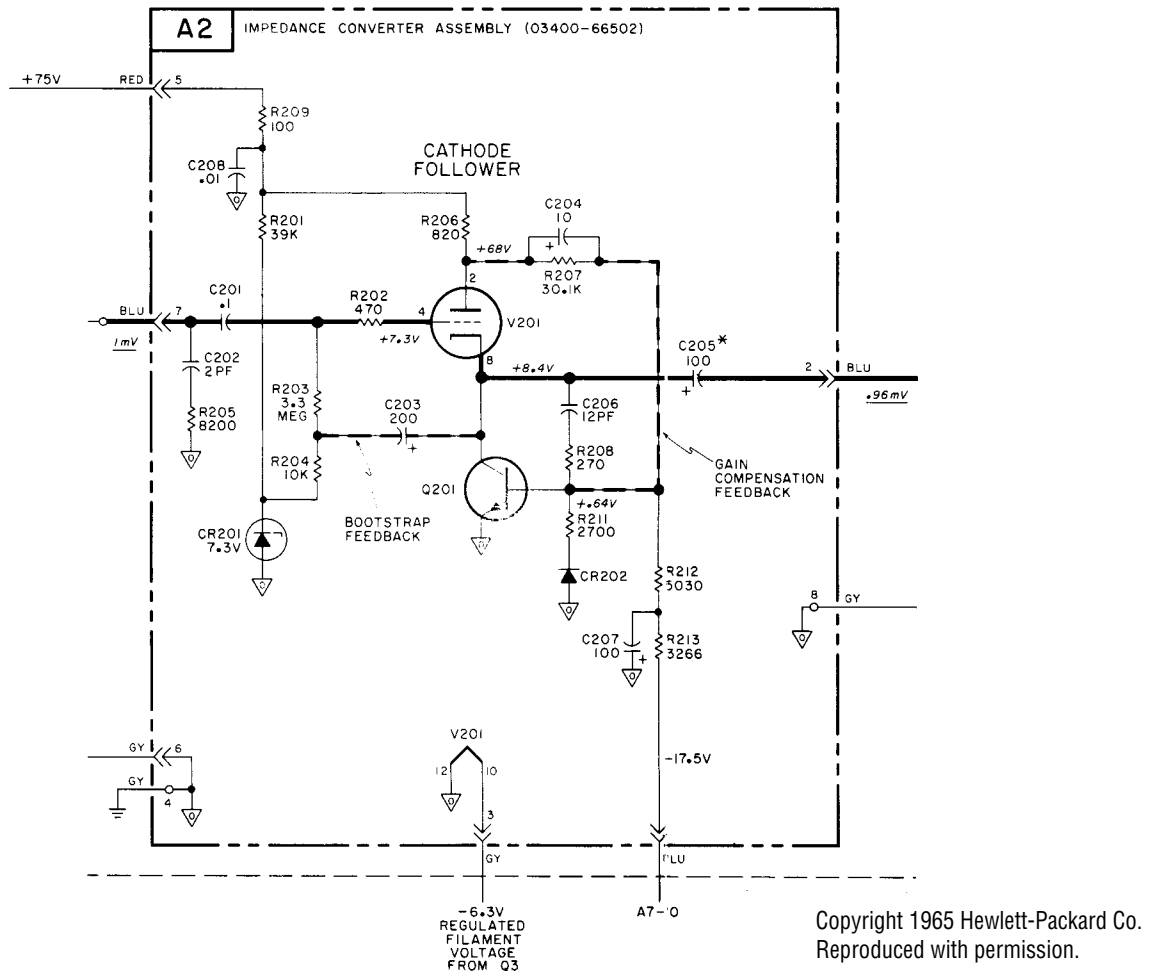


Figure A1. The "Impedance Converter Assembly," H-P's Equivalent of Figure 22's Wideband FET Buffer

Note 3: Although JFETs were available in 1965 their performance was inadequate for this design's requirements. The only available option was the Nuvistor triode described.

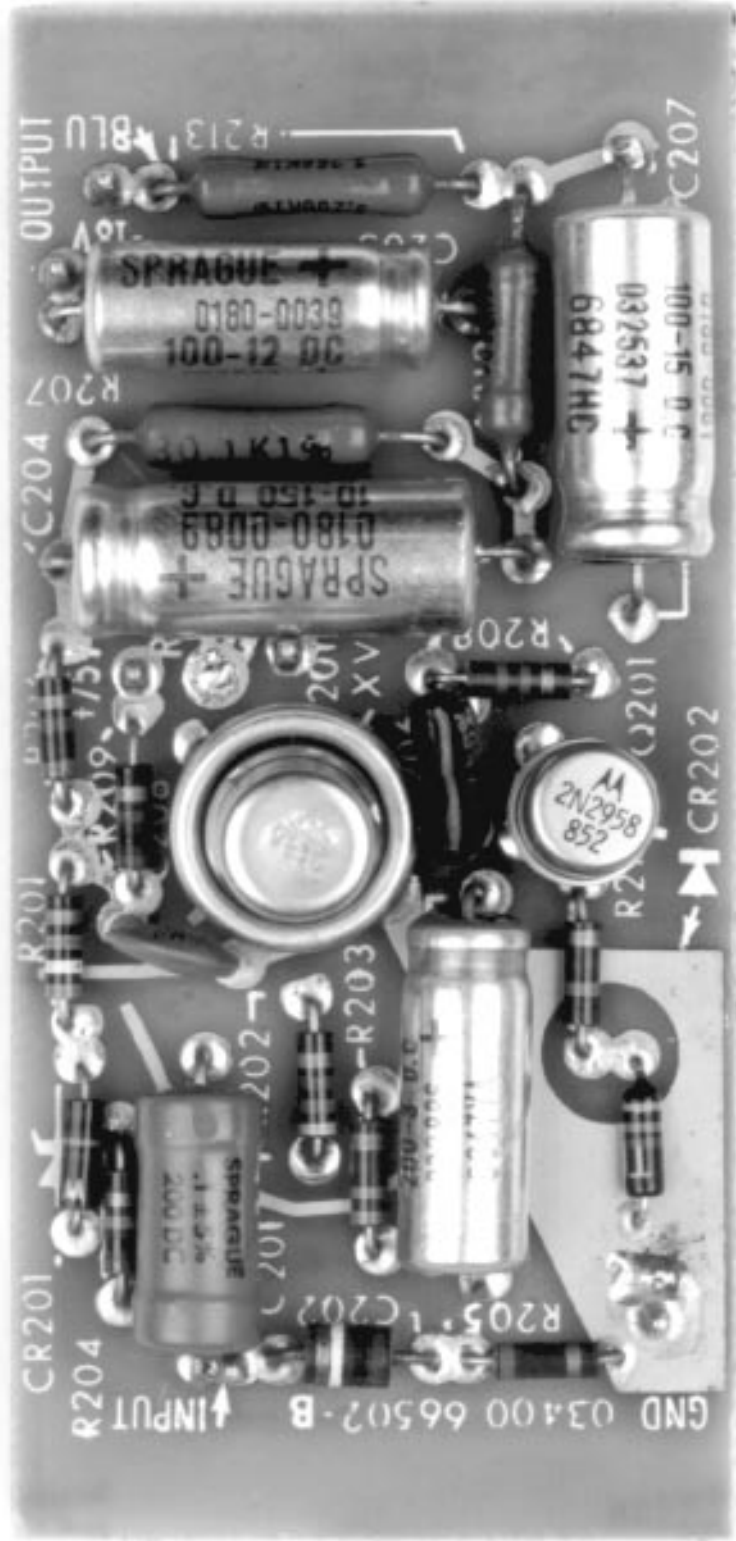


Figure A2. The Hewlett-Packard 3400A's Wideband Input Buffer. Nuvistor Triode (Upper Center) Provided Speed, Low Noise, and High Impedance. Circuit Required 75V, -17.5V and -6.3V Supplies. Regulated Filament Supply Stabilized Follower Gain While Minimizing Noise

4-22. VIDEO AMPLIFIER ASSEMBLY A4.

4-23. The video amplifier functions to provide constant gain to the ac signal being measured over the entire frequency range of Model 3400A. See video amplifier assembly schematic diagram illustrated on Figure 6-2.

4-24. The ac input signal from the second attenuator is coupled through C402 to the base of input amplifier Q401. Q401, a class A amplifier, amplifies and inverts the signal which is then direct coupled to the base of bootstrap amplifier Q402. The output, taken from Q402 emitter is applied to the base of Q403 and fed back to the top of R406 as a bootstrap feedback. This positive ac feedback increases the effective ac resistance of R406 allowing a greater portion of the signal to be felt at the base of Q402. In this manner, the effective ac gain of Q401 is increased for the mid-band frequencies without disturbing the static operating voltages of Q401.

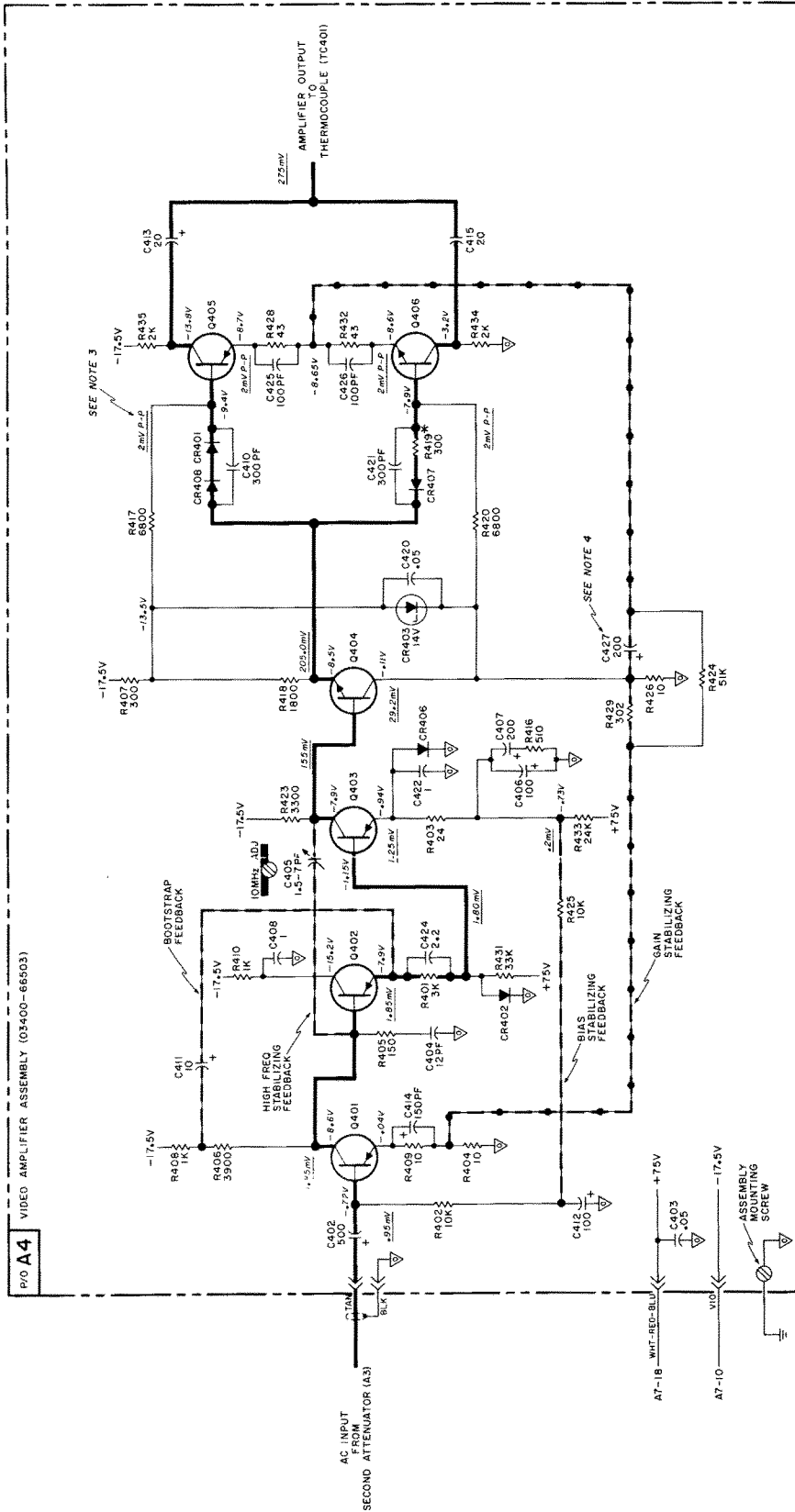
4-25. Driver amplifier Q403 further amplifies the ac signal and the output at Q403 collector is fed to the base circuit emitter follower Q404. The feedback path from the collector of Q403 to the base of Q402 through C405 (10 MHz ADJ) prevents spurious oscillations at high input frequencies. A dc feedback loop exists from the emitter circuit of Q403, to the base of Q401 through R425. This feedback stabilizes the Q401 bias voltage. Emitter follower Q404 acts as a driver for the output amplifier consisting of Q405 and Q406; a complimentary pair operating as a push-pull amplifier. The video amplifier output is taken from the collectors of the output amplifiers and applied to thermocouples TC401. A gain stabilizing feedback is developed in the emitter circuits of the output amplifiers. This negative feedback is applied to the emitter of input amplifier Q401 and establishes the overall gain of the video amplifier.

4-26. Trimmer capacitor C405 is adjusted at 10 MHz for frequency response of the video amplifier. Diodes CR402 and CR406 are protection diodes which prevent voltage surges from damaging transistors in the video amplifier. CR401, CR407, and CR408 are temperature compensating diodes to maintain the zero signal balance condition in the output amplifier over the operating temperature range. CR403, a breakdown diode, establishes the operating potentials for the output amplifier.

If that's not enough to make you propose marriage to modern high speed monolithic amplifiers, consider the design heroics spent on the thermal converter.

Copyright 1965 Hewlett-Packard Co.
Reproduced with permission.

Application Note 61



Copyright 1965 Hewlett-Packard Co.
Reproduced with permission.

Figure A3. H-P's Wideband Amplifier, the "Video Amplifier Assembly" Contained DC and AC Feedback Loops, Peaking Networks, Bootstrap Feedback and Other Subtleties to Equal Figure 22's Performance

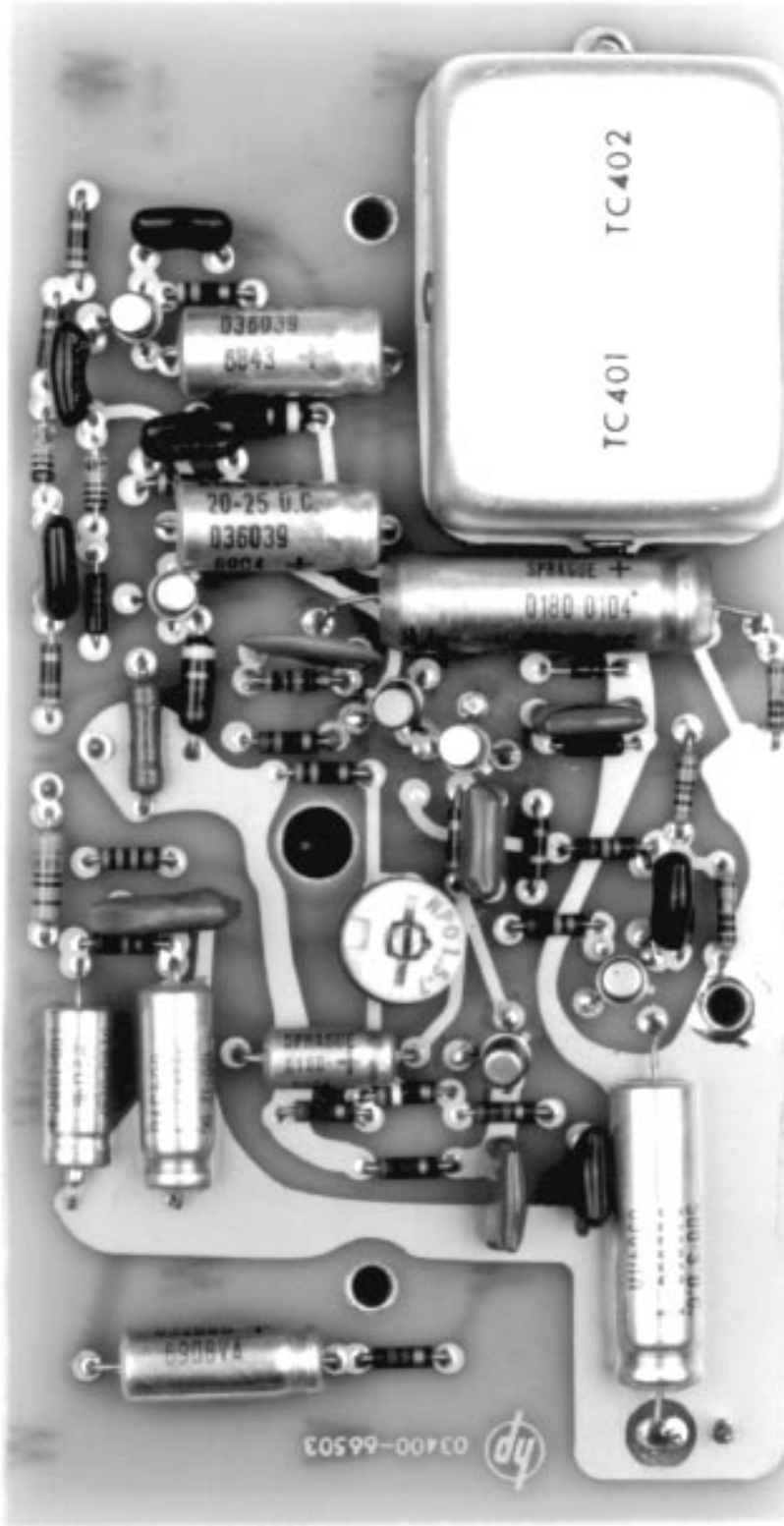


Figure A4. The Voltmeters "Video Amplifier" Received Input at Board's Left Side. Amplifier Output Drive Shrouded Thermal Converter at Lower Right. Note High Frequency Response Trimmer Capacitor at Left Center

4-27. PHOTOCHOPPER ASSEMBLY A5, CHOPPER AMPLIFIER ASSEMBLY A6, AND THERMOCOUPLE PAIR (PART OF A4).

4-28. The modulator/demodulator, chopper amplifier, and thermocouple pair form a servo loop which functions to position the direct reading meter M1 to the rms value of the ac input signal⁴. See modulator/demodulator, chopper amplifier, and thermocouple pair schematic diagram illustrated in Figure 6-3.

4-29. The video amplifier output signal is applied to the heater of thermocouple TC401. This ac voltage causes a dc voltage to be generated in the resistive portion of TC401 which is proportional to the heating effect (rms value) of the ac input. The dc voltage is applied to photocell V501.

4-30. Photocells V501 and V502 in conjunction with neon lamps DS501 and DS502 form a modulator circuit⁵. The neon lamps are lighted alternately between 90 and 100 Hz. Each lamp illuminates one of the photocells. DS501 illuminates V501; DS502 illuminates V502. When a photocell is illuminated it has a low resistance compared to its resistance when dark. Therefore, when V501 is illuminated, the output of thermocouple TC401 is applied to the input of the chopper amplifier through V501. When V502 is illuminated, a ground signal is applied to the chopper amplifier. The alternate illumination of V501 and V502 modulates the dc input at a frequency between 90 and 100 Hz. The modulator output is a square wave whose amplitude is proportional to the dc input level.

4-31. The chopper amplifier, consisting of Q601 through Q603, is a high gain amplifier which amplifies the square wave developed by the modulator. Power supply voltage variations are reduced by diodes CR601 thru CR603. The amplified output is taken from the collector of Q603 and applied to the demodulator through emitter follower Q604.

4-32. The demodulator comprises two photocells, V503 and V504, which operate in conjunction with DS501 and DS502; the same neon lamps used to illuminate the photocells in the modulator. Photocells V503 and V504 are illuminated by DS501 and DS502, respectively.

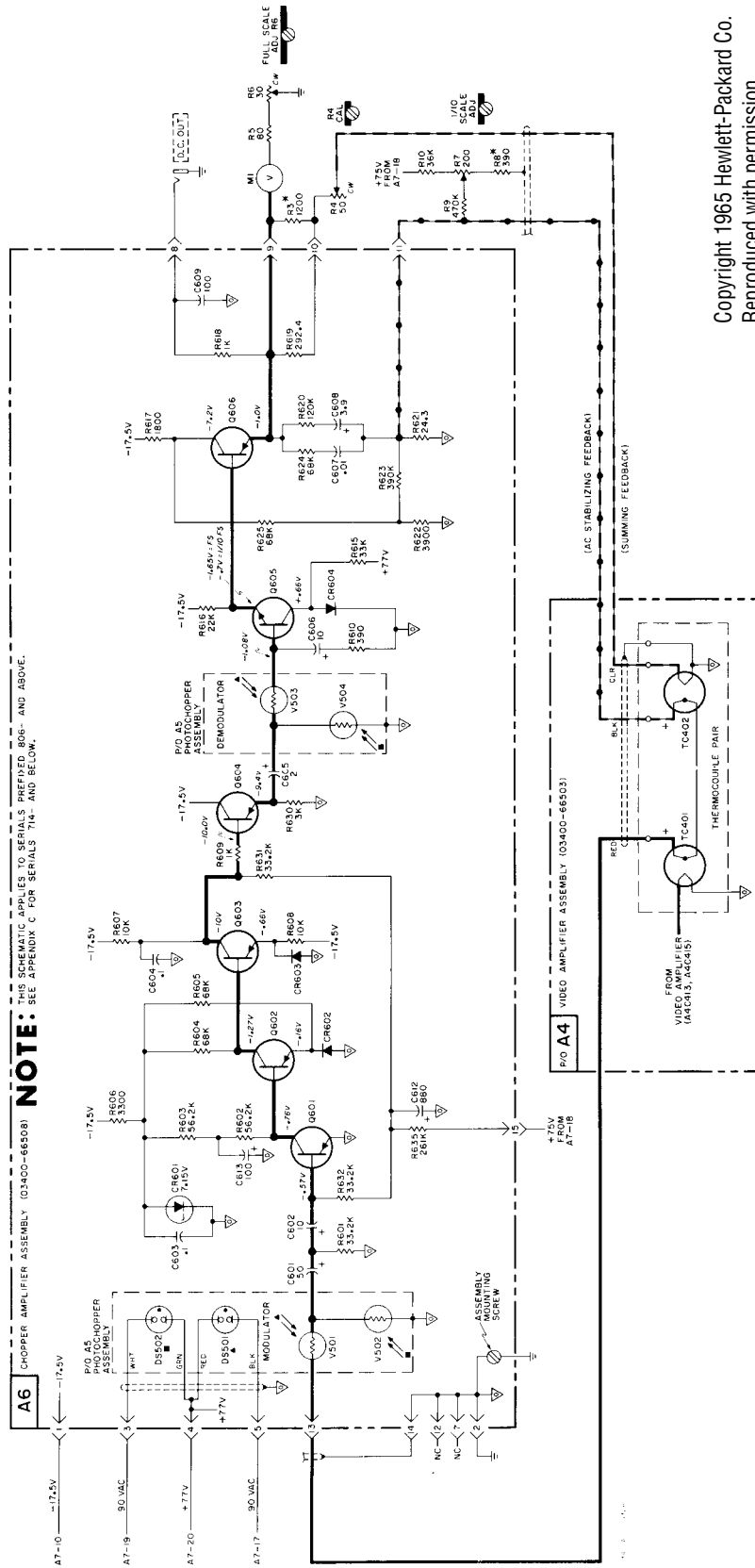
4-33. The demodulation process is the reverse of the modulation process discussed in Paragraph 4-30. The output of the demodulator is a dc level which is proportional to the demodulator input. The magnitude and phase of the input square wave determines the magnitude and polarity of the dc output level. This dc output level is applied to two emitter follower output stages.

4-34. The emitter follower is needed to match the high output impedance of the demodulator to the low input impedance of the meter and thermocouple circuits. The voltage drop across CR604 in the collector circuit of Q605 is the operating bias for Q604. This fixed bias prevents Q605 failure when the base voltage is zero with respect to ground.

Copyright 1965 Hewlett-Packard Co.
Reproduced with permission.

Note 4: In 1965 almost all thermal converters utilized matched pairs of discrete heater resistors and thermocouples. The thermocouples' low level output necessitated chopper amplifier signal conditioning, the only technology then available which could provide the necessary DC stability.

Note 5: The low level chopping technology of the day was mechanical choppers, a form of relay. H-P's use of neon lamps and photocells as microvolt choppers was more reliable and an innovation. Hewlett-Packard has a long and successful history of using lamps for unintended purposes.



Copyright 1965 Hewlett-Packard Co.
 Reproduced with permission.

Figure A5. H-P's Thermal Converter ("A4") and Control Amplifier ("A6") Perform Similarly to Text Figure 22's Dual Op Amp. Circuit Realization Required Far More Attention to Details

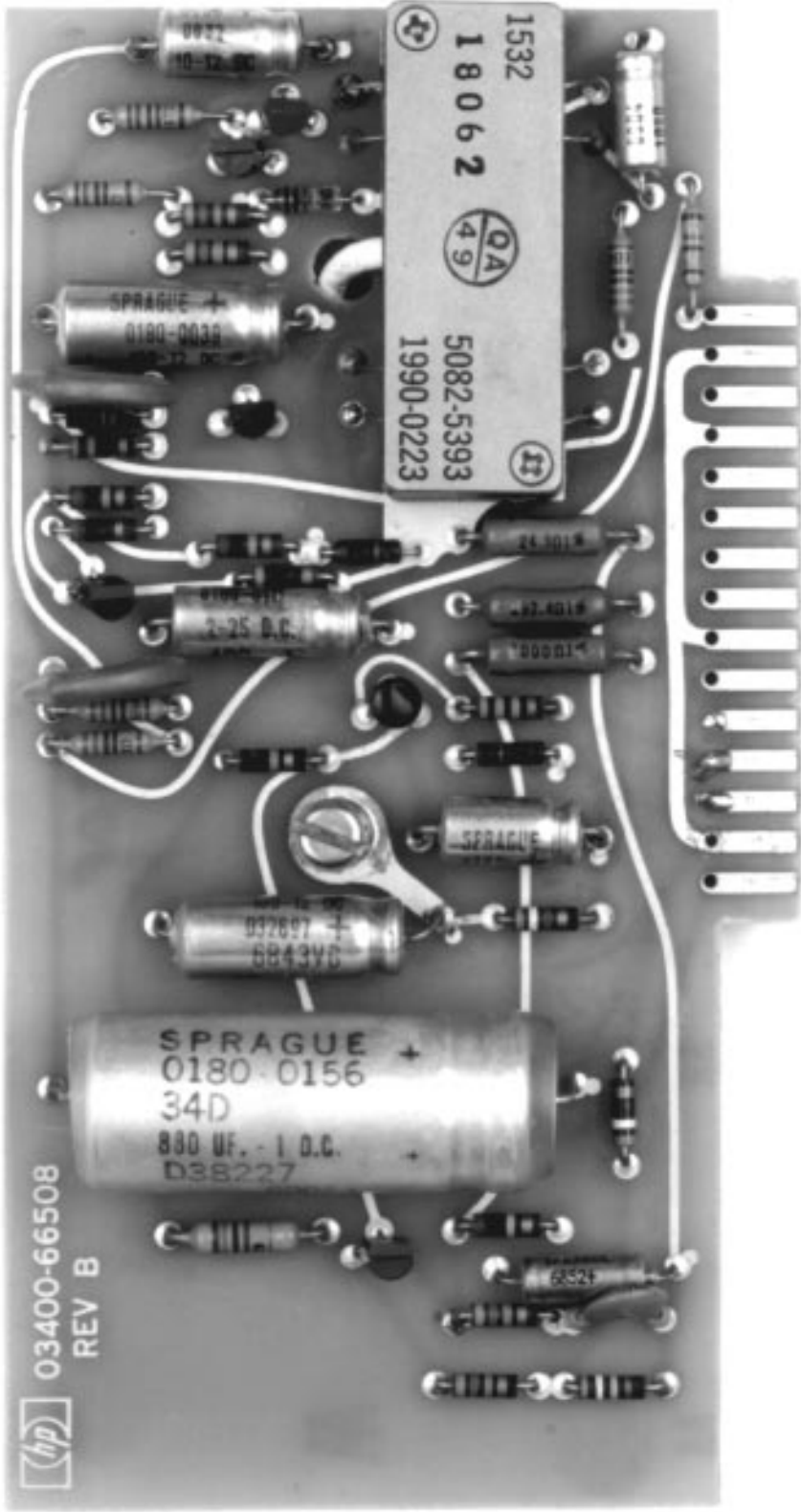


Figure A6. Chopper Amplifier Board Feedback Controlled the Thermal Converter. Over Fifty Components Were Required, Including Neon Lamps, Photocells and Six Transistors. Photo-Chopper Assembly Is at Board's Lower Right

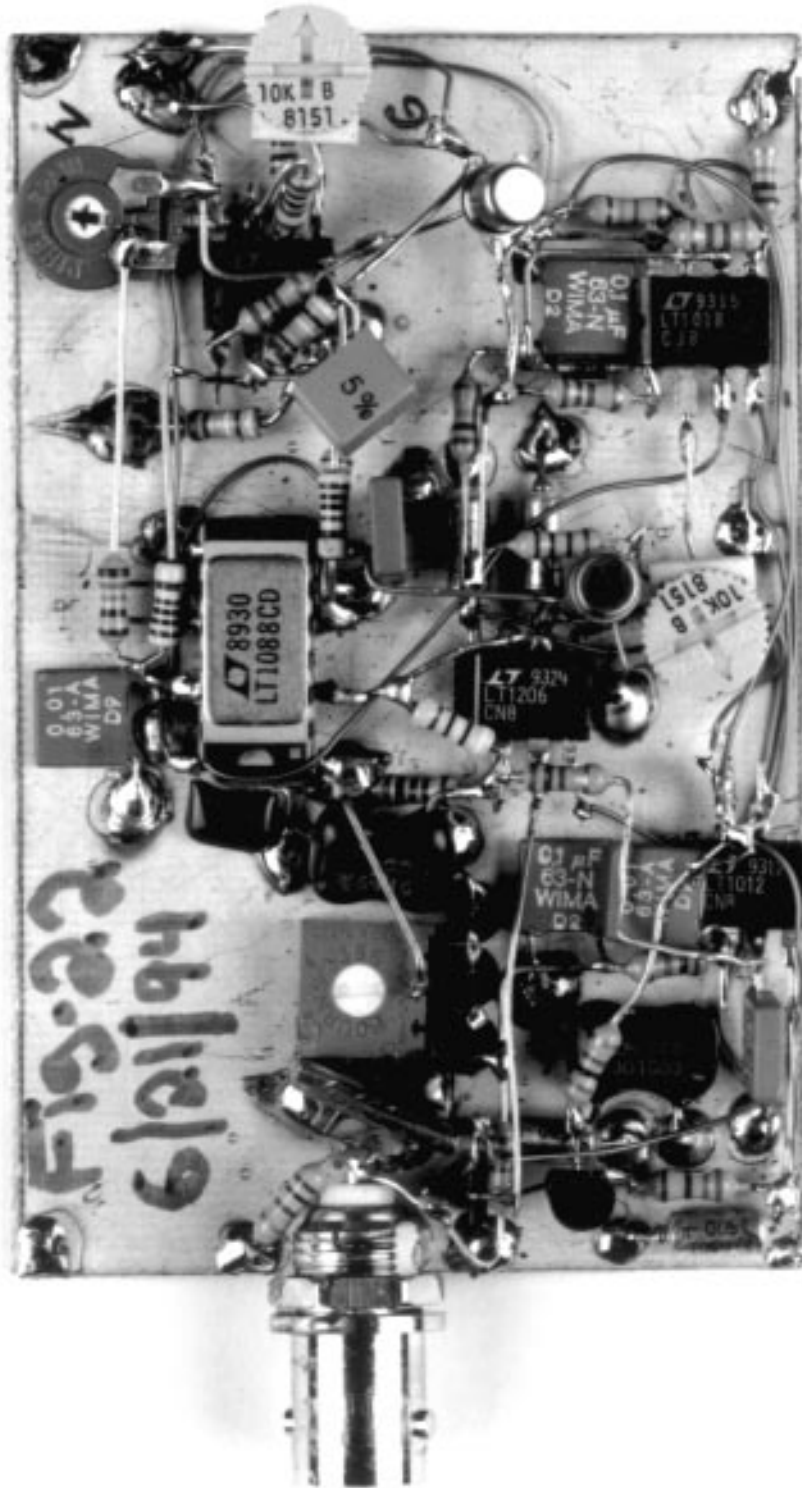


Figure A7. Figure 22's Circuit Puts Entire HP3400 Electronics on One Small Board. FET Buffer-LT1206 Amplifier Appear Left Center Behind BNC Shield. LT1088 IC (Upper Center) Replaces Thermal Converter. LT1013 (Upper Right) Based Circuitry Replaces Photo-Chopper Board. LT1018 and Components (Lower Right) Provide Overload Protection. Ain't Modern ICs Wonderful?

Application Note 61

4-35. The dc level output, taken from the emitter of Q606, is applied to meter M1 and to the heating element of thermocouple TC402. The dc voltage developed in the resistive portion of TC402 is effectively subtracted from the voltage developed by TC401. The input signal to the modulator then becomes the difference in the dc outputs of the two thermocouples. When the difference between the two thermocouples becomes zero the dc from the emitter followers (driving the meter) will be equal to the ac from the video amplifier.

4-36. Noise on the modulated square wave is suppressed by feedback from emitter of Q606 through C607 and C608 to the resistive element of TC402.

Copyright 1965 Hewlett-Packard Co. Reproduced with permission.

When casually constructing a wideband amplifier with a few mini-DIPs, the reader will do well to recall the pain and skill expended by the HP3400A's designers some 30 years ago.

Incidentally, what were *you* doing in 1965?

APPENDIX B

Symmetrical White Gaussian Noise

by Ben Hessen-Schmidt,
NOISE COM, INC.

White noise provides instantaneous coverage of all frequencies within a band of interest with a very flat output spectrum. This makes it useful both as a broadband stimulus and as a power-level reference.

Symmetrical white Gaussian noise is naturally generated in resistors. The noise in resistors is due to vibrations of the conducting electrons and holes, as described by Johnson and Nyquist.¹ The distribution of the noise voltage is symmetrically Gaussian, and the average noise voltage is:

$$\bar{V}_n = 2\sqrt{kT \int R(f) p(f) df} \quad (1)$$

Where:

- k = 1.38E-23 J/K (Boltzmann's constant)
- T = temperature of the resistor in Kelvin
- f = frequency in Hz
- h = 6.62E-34 Js (Planck's constant)
- R(f) = resistance in ohms as a function of frequency

$$p(f) = \frac{hf}{kT[\exp(hf/kT) - 1]} \quad (2)$$

Note 1: See "Additional Reading" at end of this section.

$p(f)$ is close to unity for frequencies below 40GHz when T is equal to 290°K. The resistance is often assumed to be independent of frequency, and $\int df$ is equal to the noise bandwidth (B). The available noise power is obtained when the load is a conjugate match to the resistor, and it is:

$$N = \frac{\bar{V}_n^2}{4R} = kTB \quad (3)$$

where the "4" results from the fact that only half of the noise voltage and hence only 1/4 of the noise power is delivered to a matched load.

Equation 3 shows that the available noise power is proportional to the temperature of the resistor; thus it is often called thermal noise power, Equation 3 also shows that white noise power is proportional to the bandwidth.

An important source of symmetrical white Gaussian noise is the noise diode. A good noise diode generates a high level of symmetrical white Gaussian noise. The level is often specified in terms of excess noise ratio (ENR).

$$\text{ENR (in dB)} = 10\text{Log} \frac{(T_e - 290)}{290} \quad (4)$$

T_e is the physical temperature that a load (with the same impedance as the noise diode) must be at to generate the same amount of noise.

The ENR expresses how many times the effective noise power delivered to a non-emitting, nonreflecting load exceeds the noise power available from a load held at the reference temperature of 290°K (16.8°C or 62.3°F).

The importance of high ENR becomes obvious when the noise is amplified, because the noise contributions of the amplifier may be disregarded when the ENR is 17dB larger than the noise figure of the amplifier (the difference in total noise power is then less than 0.1dB). The ENR can easily be converted to noise spectral density in dBm/Hz or $\mu\text{V}/\sqrt{\text{Hz}}$ by use of the white noise conversion formulas in Table 1.

Table 1. Useful White Noise conversion

dBm	=	dBm/Hz + 10log (BW)
dBm	=	20log (\bar{V}_n) – 10log(R) + 30dB
dBm	=	20log(\bar{V}_n) + 13dB for R = 50Ω
dBm/Hz	=	20log($\mu\bar{V}_n\sqrt{\text{Hz}}$) – 10log(R) – 90dB
dBm/Hz	=	–174dBm/Hz + ENR for ENR > 17dB

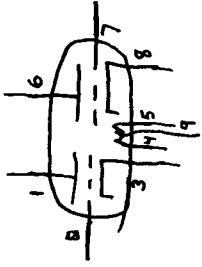
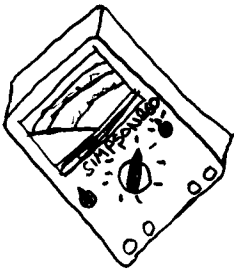
When amplifying noise it is important to remember that the noise voltage has a Gaussian distribution. The peak voltages of noise are therefore much larger than the average or RMS voltage. The ratio of peak voltage to RMS voltage is called crest factor, and a good crest factor for Gaussian noise is between 5:1 and 10:1 (14 to 20dB). An amplifier's 1dB gain-compression point should therefore be typically 20dB larger than the desired average noise-output power to avoid clipping of the noise.

For more information about noise diodes, please contact NOISE COM, INC. at (201) 261-8797.

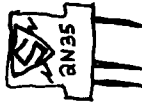
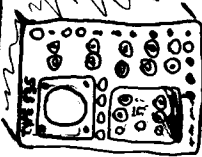
Additional Reading

1. Johnson, J.B, "Thermal Agitation of Electricity in Conductors," *Physical Review*, July 1928, pp. 97-109.
2. Nyquist, H. "Thermal Agitation of Electric Charge in Conductors," *Physical Review*, July 1928, pp. 110-113.

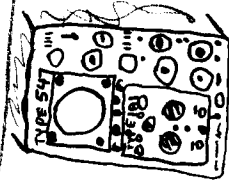
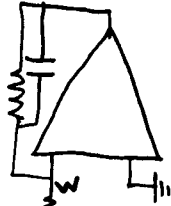
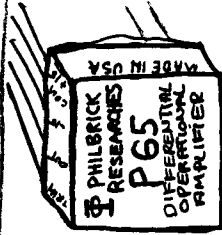
When I WAS 6 YEARS OLD
 ALL I WANTED TO DO WAS MAKE
 CIRCUITS WITH 12AX7s & 6L6s.



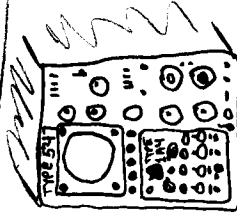
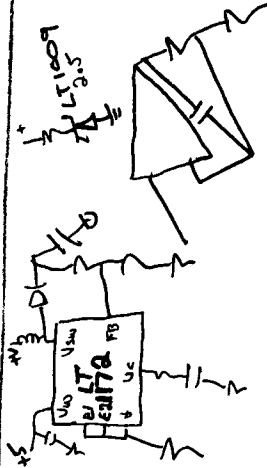
When I WAS 10 I got
 2N35s & CK-722s.
 No Filaments. wow!



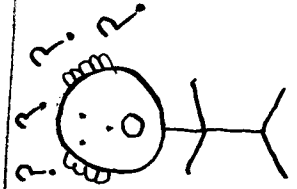
When I WAS 17 I used
 Philbrick P-65s. You
 could do anything



Now, I'm 46 & I CAN HACK
 ALL the op-amps and switching
 Regulators I WANT. EVERY DAY!



Is The Mid-Life Crisis when They
 Run out of 10K Resistors?



www.94